

The role of primary and secondary transmission on the  
dynamics of cholera in endemic areas

by

Diego Hernán Ruiz Moreno

A dissertation submitted in partial fulfillment  
of the requirements for the degree of  
Doctor of Philosophy  
(Ecology and Evolutionary Biology)  
in The University of Michigan  
2009

Doctoral Committee:

Professor Mercedes Pascual, Chair  
Professor Daniel G. Brown  
Professor Earl E. Werner  
Assistant Professor Aaron A. King

## Table of Contents

List of Figures .....	iii
List of Tables .....	v
Chapter 1. Introduction .....	1
Chapter 2. Cholera seasonality in Madras (1901-1940): A dual role for rainfall in endemic and epidemic regions.....	17
Chapter 3. Spatial clustering in the spatio-temporal dynamics of endemic cholera.....	47
Chapter 4. A metapopulation approach for cholera dynamics in endemic areas.....	79
Chapter 5. Conclusion.....	110

## List of Figures

Figure 2.1: Graphical model showing the influence of water depth on the two routes of transmission proposed for cholera .....	34
Figure 2.2: The Madras Presidency with its 26 districts.....	35
Figure 2.3: The upper panels shows monthly cholera mortality from 1901 to 1940 for two representative districts for the two regions identified in this work.....	36
Figure 2.4: Spatial correlogram for cholera mortality in Madras computed from the mean value of cholera mortality per district and the distance between the district's centroids.....	38
Figure 2.5: The LISA index applied to the coefficient of cross-correlation between cholera and rainfall (for zero lag).....	39
Figure 2.6: The LISA index applied to the coefficient of cross-correlation between cholera and rainfall for different time lags (whit cholera behind rainfall).....	41
Figure 2.7: Critical Community Size, showing the number of fade-outs for the different districts against their population density [ $h/km^2$ ].....	42
Figure 2.8: The spatial distribution of the average number of fade-outs and rainfall peaks per year.....	43
Figure 3.1: Study Area.....	64
Figure 3.2: Temporal Dynamics of Cholera epidemics.....	65
Figure 3.3: Ripley's L function for a particular epidemic.....	66
Figure 3.4: Cholera Seasonality.....	68
Figure 3.5: Cluster size for the different epidemics.....	69
Figure 3.6: Temporal dynamics of clustering and epidemic size.....	70
Figure 3.7: distribution of cluster sizes for different strains.....	71
Figure 3.S1: Clustering Size.....	73
Figure 3.S2: Clustering Size.....	74
Figure 4.1: Spatial distribution of cholera cases during the period of study.....	99
Figure 4.2: Temporal distribution of cases.....	100

Figure 4.3: Each MCMC step involves moving from a state $n$ (a set of parameters values and a sequence of events) to the next state $n+1$ .....	101
Figure 4.4: Creation of a new sequence.....	102
Figure 4.5: Average number of cases and seasonal forcing for primary and secondary transmission.....	103
Figure 4.6: Force of infection for primary ( $F_p$ ) and secondary ( $F_s$ ) transmission.....	104

## List of Tables

Table 2.1: Number of meteorological stations per district.....	32
Table 2.2: Moran's Index for the different variables.....	33
Table 3.1: Presence of significant clustering for cases.....	63
Table 3.2: Presence of significant clustering for cases-water.....	63
Table 3.S1: Results for Kruskal-Wallis test for different time aggregation of the data, showing the difference between the distribution of cases during the fall $[0 - 2\pi]$ and in the spring $[\pi - 4\pi]$ .....	72
Table 4.1: Models' Descriptions.....	96
Table 4.2: DIC and mean parameters values obtained.....	98

## **Chapter 1.**

### **Introduction**

Infectious diseases are responsible for some of the darkest chapters in human history. The “Plague of Athens” (430–427 BC), “Antonine Plague” (165-180 BC), the “Black Death” (14<sup>th</sup> century), are a few examples of events that had not only devastating effects on human population, but also contributed to shaping History itself. No wonder why infectious diseases were, and still are, a source of fear and superstition. Late in the 17<sup>th</sup> century, the unchallenged theory of spontaneous generation of diseases started to shatter when improvements in microscopy lead to the discovery of microorganisms, and thus the germ theory, or pathogenic theory of medicine developed and became the cornerstone of modern medicine and clinical microbiology. Since then, the dynamics of infectious diseases had been seen as the study of ecological interactions between pathogens and hosts. The results of these studies helped to understand and control infectious diseases in the developed world, but several diseases are still important threats in the developing world. In particular, an old disease like cholera threatens human populations in several countries in Asia and Africa, where recurrent epidemics exhibiting complex patterns require further understanding before successful control measures can be implemented.

Mathematical models for epidemiology [1], lead to the concept of infectious diseases as a dynamic process where parasites flow from one host to next. As a result, lead by the notorious contributions of Bailey [2], Ross, Snow [3], Hammer, Bartlett [4, 5] among others, the dynamics of diseases became a central topic of study. However, only after the early work of Anderson and May [6], the relationship between parasite and host was understood as an integral part of host population dynamics. Extensive time series, usually unavailable, are often the only way to identify and interpret the temporal patterns of host and parasite populations. Consequently, only during the last thirty years when the availability of detailed datasets describing temporally and spatially the dynamics of diseases had increased, a second wave of works that generated a deeper understanding of the disease processes started to be produced [7]. Ranging from simple to very sophisticated, mathematical models for infectious diseases played a critical role both in prediction and improving the understanding of diseases, with a particular (but not exclusive) interest on human disease outbreaks [8].

Compartmental models, where the host population is divided into susceptible, infected and recovered individuals (but additional compartments may be included [9, 10]), first determined the existence of conditions for epidemics to occur [1, 11]. Under this framework a whole set of epidemiological data was examined and re-analyzed. Current and historic epidemics of tuberculosis, bubonic plague, measles, cholera, foot and mouth disease, malaria, dengue, Lyme disease, among others are under study to understand key characteristics that would allow controlling outbreaks. The addition of complexity (i.e.,

forcing) on the transmission term, which describes the passage from the susceptible to the infected compartment, as well as the inclusion of heterogeneities in the host population (differences in age, behavior, or patterns of aggregation, among others) and the inclusion of models for the pathogenic agent (or its vector) accounts for the complex epidemic patterns observed for different pathogens.

Seasonality, a periodic surge in incidence corresponding to some calendar period, has been one of the central aspects of the study of infectious diseases. This is because, seasonality can influence the timing and severity of outbreaks. Hence, a better understanding of the link between seasonal variations and epidemic incidence would provide help in the design of strategies to improve public health [12]. It is important to mention here that although seasonality can be purely environmental, it usually has other components (i.e., school terms, religious peregrinations, etc) [13, 14], and even interannual events can interfere with it [15]. The seasonal forcing imposed on the transmission of infectious diseases becomes particularly interesting when different routes of transmission exist. Hence, the influence on specific aspects of the mechanisms of transmission might lead to the emergence of a complex seasonal pattern. The factors defining seasonality and their effects on the transmission for a particular disease must be considered as an indivisible unit, since relatively similar diseases may exhibit almost completely different patterns [16]. A particular ongoing disease that exhibits complex seasonality, inter-annual variation, different routes of transmission and leading cause of infant mortality is cholera.



Cholera is a disease that still threatens the human population with seven pandemics recorded in the last 200 years [16]. Its occurrence is associated with poverty and poor sanitary conditions [17] currently present in several developing countries. In the near past, moreover, its geographical range had extended and nowadays; in addition to the historic endemic areas surrounding the Bay of Bengal [18], the disease is reported periodically from several countries in Africa [19-21] where it has become a major public health problem since its reintroduction in the early '70s [22, 23].

The causative agent of cholera is *Vibrio cholerae*, a motile, gram-negative curved rod bacterium that belongs to the family Vibrionaceae. *V. cholerae* is considered an autochthonous native microbial inhabitant of brackish water and estuarine ecosystems [24, 25]. Although more than 200 serogroups, classified based on the somatic O antigen, have been identified for cholera only two, O1 and O139, are pathogenic and able to cause epidemics [26]. After the ingestion of contaminated food or water, symptomatic infected individuals exhibit diarrhea (including nausea and vomiting in the most extreme cases) as a consequence of the enterotoxin produced by the bacteria when the small intestine of the host is colonized [16]. Left untreated, cholera infections may be lethal, but treatment based on fluid and electrolyte replacement reduces mortality noticeably. During the convalescent period (approximately a week long), individuals are highly infective, contaminating water (and even food) sources usually shedding the bacterium [27]. Phenotypically, *V. cholerae* O1 can be subdivided into two different biotypes, *Classical* and *El Tor* [16]. One of the differences between these biotypes is that El Tor has lower

virulence (infected are less severely ill) and it survives longer in the natural environment (i.e., it is one of the most resistant to adverse environmental conditions) [24]. Moreover, the O1 serogroup can also be subdivided into serotypes, which produce different antigenic reactions, called *Ogawa*, *Inaba*, and the extremely rare *Hikojima* [28]. All biotype-serotype combinations can be found, although empirical evidence shows that they do not usually coexist [17]. In addition, seroconversion between *Ogawa* and *Inaba* serotypes had been reported in microcosm experiments and can result from a variety of changes, but also even from a single base change [16]. *V. cholerae* O139, also known as the Bengal strain, first appeared in 1992, causing major epidemics in India, Bangladesh and other countries (Pakistan, Nepal, China, Thailand, Kazakhstan, Afghanistan, and Malaysia) [29, 30]. Although the symptoms are the same as those caused by *V. cholerae* O1 [31], the new strain does not agglutinate with O1 antiserum [32]. Genetically, *V. cholerae* O139 and *V. cholerae* O1 El Tor are nearly identical, but the former is encapsulated [28], which may improve its survival in the environment. Their similarities suggest a close relationship between them. Genetic analysis suggests the insertion of a large foreign genomic region encoding the O139-specific genes and the simultaneous deletion of most of the O1-antigen-specific gene, which could have been originated in other non pathogenic strains [33]. These findings are of major importance, documenting not only a case of horizontal gene transfer, but also suggesting that *V. cholerae* might develop resistance to vaccines through horizontal transfer of genetic material [34]. Additionally, the fact that no immunological memory existed in the human host for *V.*

*cholerae* O139, raised questions on whether the onset of a new pandemic was being observed [31, 35], however so far, cases started to diminish, originating questions on the factors controlling these outbreaks.

Although cholera can be virtually eliminated by public sewage and water treatment [17], once cholera colonized a new territory its eradication had been proven to be extremely difficult. For example, infected individuals have been reported in the last few years in Brazil, Peru and Ecuador after invasion that occurred in 1991 [36]. The relatively low efficacy of the different cholera vaccines, about 50% [37-39], make vaccination a potential tool for controlling some of the outbreaks but eradication is still a challenge.

One of the difficulties for controlling and eradicating cholera, is that the identification of an aquatic reservoir for the bacterium has been evasive. Although the survival outside the human host was proved almost three decades ago [25, 40], the bacterium is usually not detected in the interepidemic periods, even in endemic areas like Bangladesh [41], where two epidemic peaks are reported per year with the decrease coinciding with the monsoonal season [42]. Initial evidence pointed out that zooplankton and shellfish maybe playing an important role as reservoirs [43]. More strongly, evidence suggests that *V. cholerae* survives in symbiosis with the blue green algae *Anabaena* sp., in particular inside the mucilaginous sheath where it persists during the harsh environmental conditions of the interepidemic periods [44]. In agreement with this idea, Oppenheimer observed that algal concentration peaks in April and October (see Fig 6 in [44]). However,

the magnitudes of these peaks, inversely proportional to epidemic sizes, appear to point out that other factors play fundamental roles determining the final epidemic size. Some of these factors might be related with conditions of the aquatic environment, like pH. or salinity; others maybe related with the host, like behavior or immunological history (for example, the human host may avoid risky activities during the epidemic peaks or may even have developed partial immunity to the disease). A different hypothesis pointed to the role of bacteriophages in controlling the abundance of free living bacteria and thus determining the occurrence of outburst [40, 42, 45]. None of the current hypotheses fully explains the seasonality of cholera. In particular its spatial variability, with two epidemic peaks per year typically observed in endemic places, but only one peak per year observed in epidemic areas [46]. A combination of environmentally determined abundance of free living bacteria, because of both algal blooms and phage predation, and host susceptibility, biological or merely behavioral, should be considered as central factors in determining the shape of this complex seasonal pattern.

Another challenge in controlling the epidemics is the existence of two routes of transmission. Expressing the two extremes of a continuum, primary or environmental transmission of cholera is originated on contaminated water sources, and secondary or human-to-human transmission reflects the burden of the disease caused by contact between susceptible and already infected individuals [46]. Thus, typical strategies for controlling disease spread, like isolation of infected individuals, reducing the pool of susceptible individuals through vaccination or other prophylactic methods, may be

ineffective on the grounds that infective individuals provide positive feedback to the environment, with severe consequences when water distribution networks become contaminated [43, 46].

Other features (like education and hygiene) must be also studied to control efficiently the spread of cholera and/or other infectious diseases in general. An important fact here is to consider the epidemic dynamics from the point of view of metapopulations. The concept of metapopulation, a set of local populations each of which undergoes extinction and (re)colonization events, introduced by Levin in 1969, has been prolifically studied since then. From the very beginning analogies with parasitic dynamics were drawn, however the requirement of long spatio-temporal data series prevented many developments [47]. Nowadays, the notion of metapopulation dynamics of infectious diseases has been successfully applied to some epidemiological datasets (measles, phocine distemper, and foot and mouth disease among others) [8]. In the studies of measles for example, localities were defined as human settlements (villages, towns, school districts, cities), colonization events were analogous to infection events after which these localities were labeled as infected, and population extinctions were (imperfectly) mapped to the moment when the diseases vanished from the localities. Thus one of the first results was to identify the Critical Community Size [4], the population size below which the disease goes extinct between epidemics (about 250000-400000 individuals for measles in the UK).

Secondly, localities were identified or classified as sources of infection, including

big cities where the disease is mostly endemic, or sink locations, where the persistence of the disease is strongly influenced by stochasticity and dies out easily [48]. However, in situations where a different scale for the definition of local populations is taken (i.e., families or neighborhoods), the metapopulation dynamics of the disease could be more “balanced” (population sizes are very similar), and thus the dynamics would lack locations that can act only as sources of the disease. Moreover, in these cases, environmentally initiated outbreaks might play a fundamental role, since they can incorporate a mechanism for including some degree of asynchrony and also spread locally. Thus this class of models, where events are stochastically determined and spatial constraints are considered, start to play a central role not only in disease ecology, but also other areas of ecology.

In this work the dynamics of cholera epidemics is analyzed at different spatial and temporal scales. With data from both, endemic and epidemic areas, aggregated at different spatial scales hypotheses for explaining the observed patterns are explored. In particular, the role of the different routes of transmission and factors determining differential seasonalities are studied.

The second chapter focus on the dynamic of cholera in the region known as the Madras Presidency, now the south-east of India. Using monthly mortality records, in the period 1901-1940, for the historical districts in this area, both cholera seasonality and the role of rainfall as key factor are analyzed. Furthermore, both endemic and epidemic regions were identified inside this region together with a differential role of rainfall in

determining the observed cholera seasonality.

In the third chapter, the spatial distribution and spatio-temporal changes of cholera cases is analyzed using high resolution data from Matlab, Bangladesh during 1983-2004. With the aim of recovering important information on the different routes of transmission, including the role of environmental reservoirs and, analogously to other works where insights on the propagation of epidemic fronts and metapopulation behavior [49, 48, 50], the spatio-temporal patterns of high quality cholera cases is examined. Evidence for the spatial clustering of cholera cases at different temporal and spatial scales supporting an important role of secondary transmission, is shown. Moreover, spatial clustering between cases and water sources providing insights on the effective role of water reservoirs during the onset of cholera outbreaks is presented. These analyses take into account the heterogeneity of the underlying space given by the distribution of households in the landscape.

The fourth part of this work considers a natural extension of the approach presented in the previous section. Here, different models for the dynamics of cholera cases, considering groups of patrilineally related households as units, are presented. In this chapter the particular problem of unreported events (i.e., transitions from the infected to the recovered class as well as the ones from recovered to susceptible due to waning of conferred immunity) is addressed. Additional factors, like differentiation between primary and secondary transmission, seasonality, extrinsic climate influence (i.e., ENSO) and proxies that may represent different degrees of susceptibility are also considered,

increasing the complexity of the models. In concordance with previous findings, the models including an ENSO influence on the disease dynamics performed better than the other ones. In addition, a spatially restricted transmission term also improved significantly the fit, indicating the importance of social networks in the transmission of infectious diseases. Moreover, according to these models the seasonality of primary and secondary transmission is significantly different, thus supporting previous ideas where primary and secondary transmission play different roles not only during a single epidemic peak, but also in the two peaks per year that cholera exhibit in this study area.

Together, these chapters present statistical methods and theoretical approaches that increase our understanding of cholera dynamics. The identification of differential roles for primary and secondary transmission provide evidence that measures to be taken to control cholera epidemics, must take into account not only the role of contaminated water sources but also the interaction of the host population and the network of contacts. The study of this intricate network of interactions is central to determine key actions to reduced cholera outbreaks in the near future.



## References

1. Kermack WO, McKendrick AG: **A Contribution to the Mathematical Theory of Epidemics**. *Proceedings of the Royal Society of London. Series A, Containing Papers of a Mathematical and Physical Character* 1927, **115**:700-721.
2. Bailey NTJ: *The Mathematical Theory of Infectious Diseases and Its Applications*. 1st edition. 1957:413.
3. Snow J: *On the mode of communication of cholera*. London: John Churchill, New Burlington Street, England; 1855:139.
4. Bartlett MS: **Measles Periodicity and Community Size**. *Journal of the Royal Statistical Society. Series A (General)* 1957, **120**:48-70.
5. Bartlett MS: **The Critical Community Size for Measles in the United States**. *Journal of the Royal Statistical Society. Series A (General)* 1960, **123**:37-44.
6. Anderson RM, May RM: **Regulation and Stability of Host-Parasite Population Interactions: I. Regulatory Processes**. *The Journal of Animal Ecology* 1978, **47**:219-247.
7. Smith KF, Dobson AP, McKenzie FE, et al.: **Ecological theory to enhance infectious disease control and public health policy**. *Frontiers in Ecology and the Environment* 2005, **3**:29-37.
8. Keeling MJ, Rohani P: *Modeling Infectious Diseases in Humans and Animals*. 1st edition. Princeton University Press; 2007.
9. Wearing HJAR: **Appropriate Models for the Management of Infectious Diseases**. *PLoS Medicine* 2005, **2**:e174.
10. Keeling MJ, Grenfell BT: **Understanding the persistence of measles: reconciling theory, simulation and observation**. *Proc. Biol. Sci* 2002, **269**:335-343.
11. Hudson PJ, Rizzoli A, Grenfell BT, Heesterbeek H, Dobson AP: *The Ecology of Wildlife Diseases*. 1st edition. Oxford University Press, USA; 2002.
12. Altizer S, Dobson A, Hosseini P, et al.: **Seasonality and the dynamics of infectious diseases**. *Ecol Lett* 2006, **9**:467—484.

13. [Anonymous]: **Indian pilgrimages and cholera.** *British Medical Journal* 1927, **1927**:346-347.
14. Fine PEM, Clarkson JA: **Measles in England and Wales--I: An Analysis of Factors Underlying Seasonal Patterns.** *Int. J. Epidemiol.* 1982, **11**:5-14.
15. Koelle K, Rodo X, Pascual M, Yunus M, Mostafa G: **Refractory periods and climate forcing in cholera dynamics.** *Nature* 2005, **436**:696—700.
16. Kaper JB, Morris JG, Levine MM: **Cholera.** *Clinical Microbiology Reviews* 1995, **8**:48—86.
17. Pollitzer R: *Cholera.* World Health Organization; 1959:—.
18. Russell AJH: **A statistical approach to the epidemiology of cholera in Madras Presidency.** *Proceedings Of The National Academy Of Sciences USA* 1925, **11**:653—657.
19. Luque Fernández MÁ, Bauernfeind A, Jiménez JD, et al.: **Influence of temperature and rainfall on the evolution of cholera epidemics in Lusaka, Zambia, 2003-2006: analysis of a time series.** *Transactions of the Royal Society of Tropical Medicine and Hygiene* 2009, **103**:137-143.
20. Mintz ED, Guerrant RL: **A Lion in Our Village -- The Unconscionable Tragedy of Cholera in Africa.** *N Engl J Med* 2009, **360**:1060-1063.
21. Smith A, Keddy K, De Wee L: **Characterization of Cholera Outbreak Isolates from Namibia, December 2006 to February 2007.** *Epidemiology and Infection* 2008, **136**:1207-1209.
22. Glass R, Claeson M, Blake P, Waldman R, Pierce N: **Cholera in Africa - Lessons on transmission and control for Latin-America.** *Lancet* 1991, **338**:791-795.
23. Kwofie K: **Spatio-Temporal analysis of cholera diffusion in western Africa.** *Economic Geography* 1976, **52**:127-135.
24. Lee K: **The Global Dimensions of Cholera.** *Global Change & Human Health* 2001, **2**:6-17.
25. Xu H, Roberts N, Singleton FL, et al.: **Survival and viability of nonculturable Escherichia coli and Vibrio cholerae in the estuarine and marine environment.**

*Microbial Ecology* 1982, **8**:313-323.

26. Sack DA, Sack RB, Nair GB, Siddique AK: **Cholera**. *The Lancet* 2004, **363**:223—233.

27. Faruque SM, Albert MJ, Mekalanos JJ: **Epidemiology, Genetics, and Ecology of Toxigenic *Vibrio cholerae***. *Microbiol. Mol. Biol. Rev.* 1998, **62**:1301-1314.

28. Uma G, Chandrasekaran M, Takeda Y, Nair GB: **Recent advances in cholera genetics**. *Current Science* 2003, **85**:1538—1545.

29. Faruque SM, Sack DA, Sack RB, et al.: **Emergence and evolution of *Vibrio cholerae* O139**. *Proceedings Of The National Academy Of Sciences USA* 2003, **100**:1304—1309.

30. Siddique A, Zaman K, Akram K, et al.: **Emergence of a new epidemic strain of *Vibrio cholerae* in Bangladesh - An epidemiologic study**. *Tropical and geographical Medicine* 1994, **46**:147-150.

31. Swerdlow DL, Ries AA: ***Vibrio cholerae* non-O1 - The eighth pandemic?** *The Lancet* 1993, **342**:382—383.

32. Ghosh AR, Koley H, De D, et al.: **Incidence and toxigenicity of *Vibrio cholerae* in a freshwater lake during the epidemic of cholera caused by serogroup O139 Bengal in Calcutta, India**. *Fems Microbiology Ecology* 1994, **14**:285—292.

33. Faruque SM, Mekalanos JJ: **Pathogenicity islands and phages in *Vibrio cholerae* evolution**. *Trends In Microbiology* 2003, **11**:505—510.

34. Campos L, Zahner V, Avelar K, et al.: **Genetic diversity and antibiotic resistance of clinical and environmental *Vibrio cholerae* suggests that many serogroups are reservoirs of resistance**. *Epidemiology and infection* 2004, **132**:985-992.

35. Siddique A, Akram K, Zaman K, et al.: ***Vibrio cholerae* O139: How great is the threat of a pandemic?** *Tropical Medicine & International Health* 1996, **1**:393-398.

36. Pan American Health Organization: **Number of Cholera Cases in the Americas (1990-2006)**. 2007.

37. Ali M, Emch M, von Seidlein L, et al.: **Herd immunity conferred by killed oral**

- cholera vaccines in Bangladesh: a reanalysis.** *The Lancet* 2005, **366**:44-49.
38. Clemens JD, Sack DA, Harris JR, et al.: **Field trial of oral cholera vaccines in Bangladesh.** *Lancet* 1986, **2**:124-7.
39. Clemens JD, Sack DA, Harris JR, et al.: **Field trial of oral cholera vaccines in Bangladesh: results from three-year follow-up.** *Lancet* 1990, **335**:270-3.
40. Faruque SM, Islam MJ, Ahmad QS, et al.: **Self-limiting nature of seasonal cholera epidemics: Role of host-mediated amplification of phage.** *Proceedings Of The National Academy Of Sciences USA* 2005, **102**:6119—6124.
41. Alam M, Hasan NA, Sadique A, et al.: **Seasonal Cholera Caused by *Vibrio cholerae* Serogroups O1 and O139 in the Coastal Aquatic Environment of Bangladesh.** *Appl. Environ. Microbiol.* 2006, **72**:4096-4104.
42. Faruque SM, Naser BI, Islam MJ, et al.: **Seasonal epidemics of cholera inversely correlate with the prevalence of environmental cholera phages.** *Proceedings of the National Academy of Sciences USA* 2005, **102**:1702—1707.
43. Swerdlow DL, Greene KD, Tauxe RV, et al.: **Waterborne transmission of epidemic cholera in Trujillo, Peru: lessons for a continent at risk.** *The Lancet* 1992, **340**:28-32.
44. Islam MS, Drasar BS, Sack RB: **Probable role of blue-green algae in maintaining endemicity and seasonality of cholera in Bangladesh: a hypothesis.** *J Diarrhoeal Dis Res* 1994, **12**:245-56.
45. King AA, Ionides EL, Pascual M, Bouma MJ: **Inapparent infections and cholera dynamics.** *Nature* 2008, **454**:877—880.
46. Codeço CT: **Endemic and epidemic dynamics of cholera: the role of the aquatic reservoir.** *BMC Infectious Diseases* 2001, **1**:1—1.
47. Grenfell BT, Harwood J: **(Meta)population dynamics of infectious diseases.** *Trends In Ecology & Evolution* 1997, **12**:395—399.
48. Grenfell BT, Bjørnstad ON, Kappey J: **Travelling waves and spatial hierarchies in measles epidemics.** *Nature* 2001, **414**:716—723.
49. Smith DL, Lucey B, Waller LA, Childs JE, Real LA: **Predicting the spatial**

**dynamics of rabies epidemics on heterogeneous landscapes.** *Proceedings of the National Academy of Sciences* 2002, **99**:3668—3672.

50. Russell CA, Smith DL, Childs JE, Real LA: **Predictive Spatial Dynamics and Strategic Planning for Raccoon Rabies Emergence in Ohio.** *PLoS Biology* 2005, **3**:e88—.

## **Chapter 2.**

### **Cholera seasonality in Madras (1901-1940):**

#### **A dual role for rainfall in endemic and epidemic regions**

##### **Introduction**

An understanding of the seasonality of cholera is still elusive despite the long history of descriptions of the patterns in different parts of the world and different regions of its center of endemism on the Indian sub-continent. Within regions, cholera cases can exhibit different seasonal patterns at different locations, including variations in the number of outbreaks and different delays with respect to peaks in rainfall and temperature. These patterns are not well understood because environmental drivers themselves are poorly defined for the seasonal cycle of the disease. Two peaks per year is the typical pattern described for cholera in Bangladesh and former Bengal, with a decline in the summer during the monsoons, while only one peak coincident with the rainy season is present in other regions of former British India and contemporary Brazil [1, 2]. Despite these complexities, a better understanding of cholera's seasonality is key to identify and understand the regional mechanisms behind the described influence of the El Niño Southern Oscillation (ENSO) [3-5]. It is also fundamental to build scenarios for cholera with global change. This is because both, climate variability (ENSO) and climate

change, are likely to act on infectious disease dynamics through the modulation of the seasonal cycle and modification of the seasonal times when it crosses environmental thresholds [6].

The importance of rainfall as a driver of the seasonal cycle of cholera is implied by its water-borne transmission, the dose-dependent nature of infection, and the decline of cases during the monsoon season [2]. Rainfall as a driver is also intimately connected with the two routes of transmission described for cholera in the literature [7]. Studies in volunteers have confirmed that ingestion of a dose between  $10^7$  and  $10^{11}$  is required to develop an infection [8]. Brackish waters and estuaries provide suitable environmental conditions for the bacterium to survive outside the human host [9]. In these aquatic free-living environments, both pathogenic and non-pathogenic *V. cholerae* survive in free-living states as well as attached to invertebrates and algae in the plankton [10, 11]. Thus, primary transmission presumably occurs from a reservoir of the pathogen, *V. cholerae*, in the aquatic environment. A more direct transmission route, known as secondary or “human-to-human” transmission, is mediated by the ingestion of fecally contaminated water or food [12, 7]. The relative importance of these two routes of transmission has been highly debated since early times when “contagionists” emphasized the role of human contact while “localists” focused on geography and the environment [2]. The importance of “human-to-human” transmission is supported by recent time series models fitted to the endemic dynamics of cholera in Bangladesh [3, 4]. In these, there is a clear feedback between present and past levels of infection in the population. The existence of a

short-lived hyper-infective stage provides one mechanism enhancing this transmission route [13, 14]. Clearly, the categorization of the two transmission pathways is a simplification that considers the two extremes of a continuum defined by the strength of the feedback between past and future cases and by different temporal scales of transmission [15]. For primary transmission, this feedback is weak (in the extreme non-existent), predominantly because the bacterium concentration in the environment is dominated by stochastic environmental drivers that influence its survival and population growth. However, at the other extreme of almost direct ‘human-to human’ transmission, the feedback is strong, whether or not transmission occurs through water in the environment, and the transmission rate is a function of the level of infection in the population.

Based on these two transmission routes, Dobson et al. (in prep.) have proposed the following mechanisms behind the bimodal seasonal pattern of cholera in Bangladesh. The first peak occurs in the spring, during the dry season when temperature warms up, because the bacterium thrives in the environment where it is also highly concentrated and human interactions with the limited water bodies available in the environment increase (i.e. strong primary transmission). The monsoons then lead to a decline in cholera in the summer, as heavy rainfall dilutes the concentration of the pathogen in the environment and favorable conditions of salinity and pH deteriorate. This dilution effect of rainfall represents a negative influence. However, a positive delayed effect would also occur, leading to an increase in cholera, when humans concentrate in the flooded landscape and



the existing sanitary conditions break down exacerbating secondary transmission (see Fig. 2.1) or when the free-living stages escape the influence of the phages that may play a major role in regulating their abundance [16].

This seasonal model provides predictions for both endemic and epidemic areas. In endemic regions, cholera should exhibit a negative association with rainfall at zero lag, largely reflecting the dilution effect, and a positive correlation at positive lags reflecting the increase in secondary transmission after the rains. However, in regions with long and sustained periods of rainfall, and consequently with low concentration of the pathogen in aquatic reservoirs, the local extinction of the disease should be more likely. Hence, frequent fade-outs and more irregular temporal patterns should be favored in regions with sustained rainfall and lower human populations. To examine these predictions, we analyze the association of cholera and rainfall in space and time, investigating also the notion of a Critical Community Size, the existence of a population threshold for disease persistence [17, 18].

The historical records for cholera mortality in the districts of former British India provide an opportunity to consider extensive temporal records across geographical regions. We focus here on the districts of the Madras Presidency, cholera and climate data for this region span both a large region of historic and present day India; they exhibit a range of seasonal cholera patterns, from regular to irregular, with one or two peaks per year. Based on cholera-rainfall associations and fade-out patterns, we describe two main district clusters corresponding respectively to “epidemic” and “endemic” regions, and

with distinct roles of rainfall. We provide evidence for the proposed positive and negative effects of rainfall in the bimodal seasonal cycle of endemic cholera. The spatio-temporal patterns of cholera mortality suggest a complex role of this environmental variable in the dynamics of the disease.

## **Methods and data**

The area studied corresponds to the region of former British India known as the Madras Presidency. The Madras Presidency included several districts in the southern region of India between latitudes  $20^{\circ}$  and  $8^{\circ}$ N and longitudes  $74^{\circ}$  and  $86^{\circ}$ E. We digitized the historical maps of the province and its 26 administrative sub-province divisions or districts (Fig. 2.2).

For each district, monthly cholera mortality data were extracted from the records (Annual yearbooks of the sanitary commissioner, Madras, printed by the superintendent, government press, Madras) from January 1892 to December 1940 and, for the same period, population sizes were obtained (from census every ten years). In addition, from January 1901 to December 1970, several meteorological stations located in the region recorded daily rainfall data (Table 2.1). We produced a monthly estimate of rainfall per district by averaging the readings of the corresponding meteorological stations while taking into consideration the historical borders of the districts. Because of the partial temporal overlap of the records, analyses requiring both datasets only included the period from January 1901 to December 1940. On the other hand, whenever cholera mortality or

rainfall were analyzed independently, the full extent of the time series was used (1892-1940 and 1901-1970 respectively).

A spatial correlogram [19, 20], for mean cholera mortality for each district and the distance between their centroids was performed to define the distance for which the disease autocorrelation decays to zero. This distance allows us to define districts that are considered neighbors and are specified as such in a proximity matrix. We used this proximity matrix to examine the spatial structure of the association between cholera and rainfall. The coefficient of cross-correlation between the cholera and rainfall time series was calculated for lags ranging from 0 to 12 months (with rainfall preceding cholera). We applied the well-known (global) autocorrelation index, Moran's I [21] to this quantity to determine the degree of clustering of the association between cholera and rainfall. To further determine the geographical location of the clusters, we applied the modification of the Moran's index known as the Local Indicator of Spatial Association, LISA [22]. Whereas Moran's I evaluates the degree of global clustering, the LISA index allows for local variation and therefore localizes "hot-spots" and "cold-spots", or clusters, with respectively high and low associations values between cholera and rainfall. To determine whether clusters in the association reflect the spatial structure of the disease itself, we applied these same indices to the mean cholera mortality per district.

The spatio-temporal dynamics of cholera mortality and the degree of spatial association can also be analyzed by looking at the synchrony of outbreaks in the Madras presidency. Synchrony between populations can be quantified with the zero-lag-cross-

correlation between the time series of log-cases evaluated against the region-wide synchrony [23]. To calculate the zero-lag-cross-correlation, we first define a new time series,  $z_t$ , which corresponds to the first-differenced time series of log-transformed cholera mortality ( i.e.,  $z_t = \log(N_t + 1) - \log(N_{t-1} + 1)$  (where a 1 has been added to handle the case of no reported deaths). The average of the cross-correlation coefficient, which is known as the region-wide synchrony, is defined as

$$average_{i \neq j}(\rho_{i,j}) = \frac{2}{N \cdot (N-1)} \cdot \sum_{i=1}^N \sum_{j=i+1}^N \rho_{i,j}$$

where  $\rho_{i,j}$  represents the cross-correlation coefficient between the time series  $z_t$  at sites  $i$  and  $j$ . Because the cross-correlation coefficients are not independent, a bootstrap confidence interval for the mean synchrony was generated using a sampling method [24]. The same analysis was applied to the rainfall data to examine whether patterns of synchrony correspond to those of rainfall.

Besides the existence of an association with rainfall, our hypothesis on cholera seasonality predicts that different patterns of disease persistence should be observed in districts with different intensity of the rainfall season. To examine this prediction, two dynamical measures were considered: the Critical Community Size and the seasonal variability of rainfall. The Critical Community Size (CCS), the population size below which a disease dies out in the troughs between epidemics, reflects the dynamics of extinction [18]. Hence, a qualitative measure of the CCS was obtained for the districts where population data were available. A period of at least two consecutive months without

mortality was considered a **fade-out**. The same qualitative results were obtained when this analysis was performed with longer and shorter periods (ranging from 1 to 6 months for the definition of a fade-out).

Rainfall patterns were first examined by themselves, and then in association with cholera cases. All the districts exhibited a high annual peak in rainfall due to the southwest monsoon [25]. When the mean and the variance of rainfall were compared among districts, no statistically significant differences were found (results not shown). However, some districts exhibited high precipitation values lasting up to 6 months, with negligible precipitation during the rest of the year, whereas other districts had shorter monsoon seasons of 3 to 4 months with a second peak of rainfall later in the year. Exceptions without this second peak are found in the districts on the Arabian Sea. Therefore, in these analyses, we focused on the length of the rainy season. By determining how many times and for how long the monthly-accumulated rainfall exceeded a threshold value—fixed at a value of 25% above the district mean—we discriminated districts with two rainfall peaks per year from those with only one. We used this classification to interpret the clustering patterns arising from the rainfall-cholera associations. Consideration of other threshold values (between 25% and 75% above the district rainfall mean) led to similar conclusions.

## **Results**

The dynamics of the disease and its seasonal cycle appear to differ across the

districts. Some districts exhibit intermittent epidemics with numerous fade-outs, while others display seasonal outbreaks every year with high persistence of the disease. Two peaks per year are typically seen in the latter, while a single peak is present for the more irregular patterns. In addition, these seasonal patterns also differ in their typical lags relative to rainfall. Figure 2.3 illustrates these patterns for two representative districts. To better understand and characterize the spatio-temporal patterns of the disease, as well as their relationship to rainfall, we begin by considering the existence of district clusters for both rainfall and cholera independently, and for their association.

Based on the result of the spatial correlogram, districts within 200 Km or less were considered as neighbors (Fig. 2.4). The values obtained for the spatial autocorrelation, measured by the global index Moran's I, indicate that there is no significant spatial clustering when both cholera mortality and rainfall are independently considered (Table 2.2). However, this index becomes significant when evaluated for the cross-correlation between these variables, providing evidence for a spatial association between cholera and rainfall (Table 2.2).

Similarly, only small clusters emerged from the analysis of the independent variables with the LISA index, while two distinct larger clusters are apparent for their cross-correlation. Specifically, the LISA index for cholera mortality delimited one small-size cluster (districts number 17, 24 and 26) with high values in the central southern part of the region under analysis, and a second cluster close to the first, also small in size (districts 15 and 18) with low values. For rainfall, a medium-size cluster (districts number

4, 5, 11 and 14) of low values appears in the central northern region. More interestingly, when the cross-correlation between cholera and rainfall at zero lag, is considered, one large cluster emerges in the northeast region for positive significant correlations (including districts 7, 8, 9, 10, 11 and 23, and denoted as *positive correlation cluster* in Fig. 2.5). A second large cluster with negative significant values is found in the central southern area (including districts 15, 16, 17, 18, 19, 21, 24, 25 and 26, and denoted as *negative correlation cluster* in Fig. 2.5). When time lags are introduced for 3 to 7 months, the main pattern is reversed: the cluster in the southern region now reflects positive associations, while the northern one exhibits negative ones (Fig. 2.6). As expected for a seasonal pattern, the same clustering patterns emerge for lags close to 12 months.

These results are corroborated by the ones on the synchrony of outbreaks. Very low synchrony is observed when both cholera and rainfall are considered separately, with only a few districts with significant zero-lag-cross-correlation values (results not shown). The lack of synchrony is consistent with the existence of two different clusters (the positive correlation cluster and the negative correlation cluster) for the association between cholera and rainfall.

We examined next whether the districts for the different clusters we have identified, exhibit different dynamic patterns of disease persistence. As expected from theoretical considerations with stochastic disease models [17, 18], patterns of persistence are influenced by population size. Fig. 2.7 shows that districts with a higher density have a lower number of fade-outs, while those with a lower density experience more frequent

fade-outs. This implies that cholera is endemic and exhibits more regular seasonality in districts with higher population densities, while outbreaks are epidemic and highly intermittent in those with lower densities. A chi-squared test comparing the distributions for the number of fade-outs between low and high density districts establishes that the differences between these districts are statistically significant (Kruskal-Wallis  $\chi^2 = 6$ , p-value = 0.01; low and high density districts are defined as those with densities between 45 and 65.7 h/Km<sup>2</sup> and 164 and 201 h/Km<sup>2</sup>, respectively).

To determine whether fade-out patterns have a spatial structure, we compared the distribution of the number of fade-outs between northern and southern districts. The 'per year' mean (total number of fade-outs divided by the length of the time series in years) in the northern districts (1.985) is significantly larger than the one for the southern districts (0.785) (Kruskal-Wallis  $\chi^2 = 5.4857$ , p-value = 0.01, Fig. 2.8). A similar geographical pattern is obtained for the distribution of the duration of fade-outs, with the northern districts exhibiting longer fade-outs than the southern ones (Kruskal-Wallis  $\chi^2 = 9$ , p-value = 0.0027).

Do these two regions with different fade-out patterns correspond to different durations of the rainfall season? Based on the distribution of the annual duration of the rainy season, we distinguished three different regions (Fig. 2.8): a northern area with a long season (districts 6, 7, 8, 9, 10, 13, 15, 20 and 23, with an average length of 4.04 months); a central area with rains of moderate length (districts 1, 2, 3, 4, 5, 11, 12, 14, 16, 19 and 21, with an average length of 2.82 month); and a southern region with two shorter



wet seasons (districts 17, 18, 22, 24, 25 and 26, with an average length of 2.3 months).

These three regions are statistically different for the length of the rainy season (Kruskal-Wallis  $\chi^2 = 14.1429$ , p-value = 0.0001694 for the comparison of regions with long and moderate rainy seasons; Kruskal-Wallis  $\chi^2 = 10.125$ , p-value = 0.001463 for regions with long and short rainy seasons; and Kruskal-Wallis  $\chi^2 = 7.1021$ , p-value = 0.007699 for regions with moderate and shorter seasons).

## **Discussion**

The above results split the Madras Presidency into two main regions with different seasonal patterns of rainfall and cholera dynamics. The southern region exhibits a seasonal disease pattern similar to the one described in the literature for former Bengal and Bangladesh [26, 27], with two peaks per year; there is however a shift in the timing of the outbreaks consistent with the earlier dominant monsoon season. This seasonal pattern is then characteristic of “endemic” regions, with regular and persistent infection, and contrasts with the more stochastic nature of “epidemic” regions, with recurrent fade-outs and only one sporadic peak coincident with the rains. These patterns in Madras can be taken as a basis to consider the seasonal patterns of cholera in other regions, including those where the disease is a public health burden today. Endemic cycles have been described for historical data in former Bengal, while epidemic patterns occurred in the dryer region of former Punjab [2]. Epidemic cycles with significant fade-outs occur in coastal regions of western Africa today [28]. Their seasonal relationship to rainfall

patterns remains to be examined and compared to our findings here.

In the southern region of Madras, fade-outs are short and infrequent, indicating a more permanent presence of the disease and the pathogen (Fig. 2.3). A negative association between cholera and rainfall is observed at zero lags reflecting the consistent decline of cases during the monsoons, in between the two peaks. For the same region, the reversal to a positive association reflects the increase in cases that follow the monsoons. These results for the southern pattern are consistent with the predictions of our seasonal model, with a “dilution” effect of rainfall on the environmental concentration of the pathogen but also an enhancing effect on secondary transmission during extreme rainfall events (Dobson et al., in prep). While the first effect has been described in the literature, the second is novel for the bimodal cholera pattern.

The northeast cluster, defined by a positive correlation with rainfall at zero lag, is mainly composed of districts with a single epidemic peak when present. These districts display longer and more frequent fade-outs (Fig. 2.3). This unimodal pattern coincident with the monsoons combined with its stochastic nature suggests that in places where secondary transmission cannot be sustained over time, an environmental reservoir of pathogenic *Vibrio cholerae* is not effectively maintained at a level sufficient to cause disease. More sustained periods of rain imply longer duration of the dilution of the pathogen concentration in aquatic reservoirs, and epidemics occur during the rainy season presumably through immigration of infected individuals and the consequent secondary route of transmission. In endemic regions, the human feedback from infected individuals

to aquatic reservoirs appears critical to sustain the so-called primary transmission.

These results underscore the complexities of the role of rainfall on the seasonal dynamics of cholera, and their dependency on the endemic vs. epidemic nature of the disease. Open questions remain on the mechanisms behind the different lags in different regions for the positive effect of rainfall on transmission. A better understanding of these different lags will require a more detailed analysis of the spatio-temporal patterns focused on the spatial propagation of the disease. In particular, mechanistic models should examine how the persistence of an environmental reservoir interacts with levels of immunity in the population in ways that may affect disease dynamics at seasonal scales. The effect of environmental water levels on the recently discovered interaction between the *V. cholerae* and phage [16] must also be examined (Dobson et al, in prep.). Both these mechanisms could affect the lag of cholera outbreaks relative to the timing of rainfall events.

The existence of both, positive and negative effects of rainfall in the seasonal cycle is consistent with the previously described associations of this variable with the transmission rate of cholera at longer temporal scales. Recent findings suggest that high precipitation and flooding mediate in part the effect of El Niño in the approximately four year cycle of the disease [4]. The same time series model indicates, however, that at even longer temporal scales, rainfall and river discharge are negatively associated with disease transmission. The complex role of water reflects multiple mechanisms and spatio-temporal scales involved in the concentration of the pathogen in the environment and in

the human behavior underlying contact with water and the pathogen itself. The seasonal model supported by these findings can be used to further investigate these mechanisms and provides a basis to build predictive models that incorporate seasonality as a function of environmental drivers.

**Table 2.1:** Number of meteorological stations per district. The rainfall data of Chingleput were used for the city of Madras.

District	Number of Meteorological Stations
Anantapur	10
Bellary	9
Chingleput	11
Chittoor	8
Cuddapah	10
Ganjam	12
Godivari East	18
Godivari West	5
Guntur	15
Kistna	9
Kurnool	9
Madras	-
Malabar	23
Nellore	14
Nilgiris	9
North Arcot	11
Ramnad	9
Salem	21
South Arcot	13
South Kanara	10
Tanjore	17
Tinnevelly	8
Vizgapatam	21
Trichinopoly	17
Coimbatore	15
Madua	10

**Table 2.2:** Moran's Index for the different variables. The p-values are indicated in parentheses.

	Mean Cholera	Mean Rainfall	Cross-correlation between Cholera and Rainfall
Moran's I	0.05 (0.187)	0.15 (0.018)	0.49 (0.001)

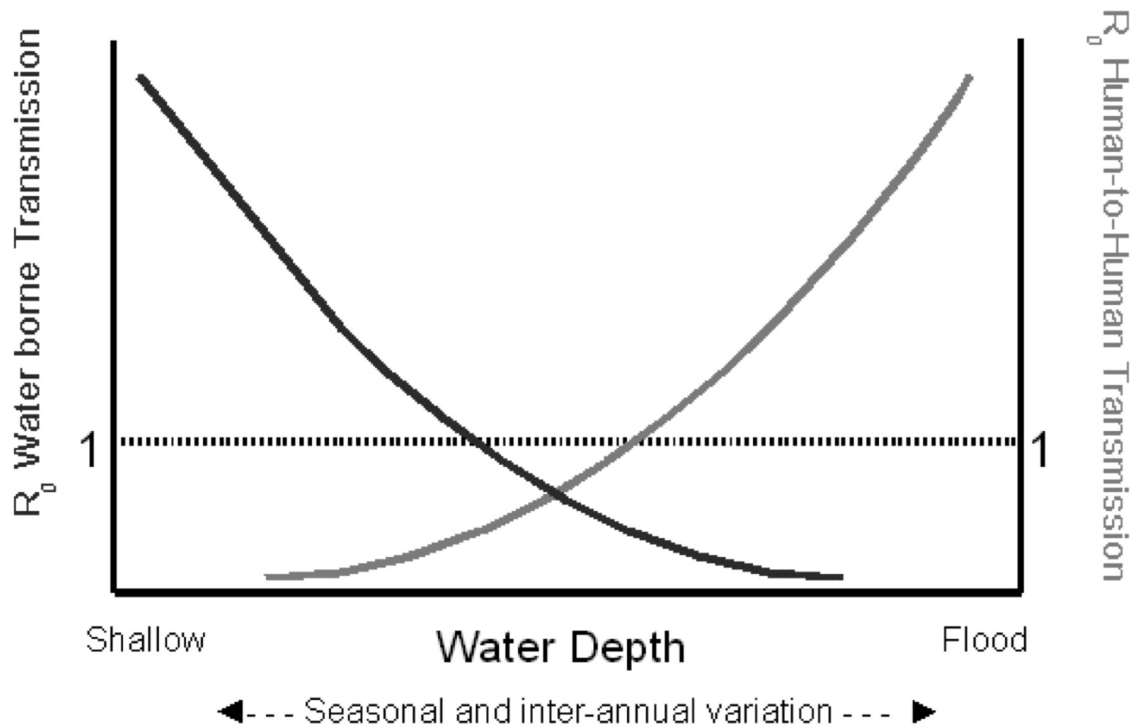


**Figure 2.1:** Graphical model showing the influence of water depth on the two routes of transmission proposed for cholera. Outbreaks occur when  $R_0 > 1$ . The dark gray line shows the decrease of primary transmission as water depth increases, while the gray line shows the increase of secondary transmission. Under shallow-water conditions, primary transmission is high, while flood conditions turn on and favor the subsequent development of secondary transmission.

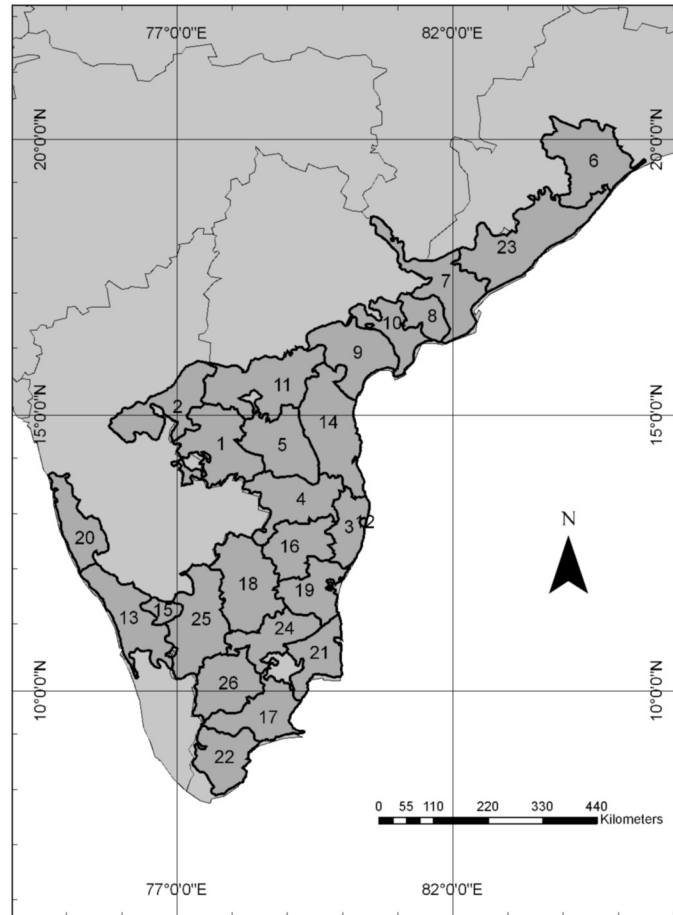


**Figure 2.2:** The Madras Presidency with its 26 districts: (1) Anantapur, (2) Bellary, (3) Chingleput, (4) Chittoor, (5) Cuddapah, (6) Ganjam, (7) Godivari East, (8) Godivari West, (9) Guntur, (10) Kistna, (11) Kurnool, (12) neighborhood of Madras, the former capital city, (13) Malabar, (14) Nellore, (15) Nilgiris, (16) North Arcot, (17) Ramnad, (18) Salem, (19) South Arcot, (20) South Kanara, (21) Tanjore, (22) Tinnevelly, (23) Vizagapatam, (24) Trichinopoly, (25) Coimbatore and (26) Madua.



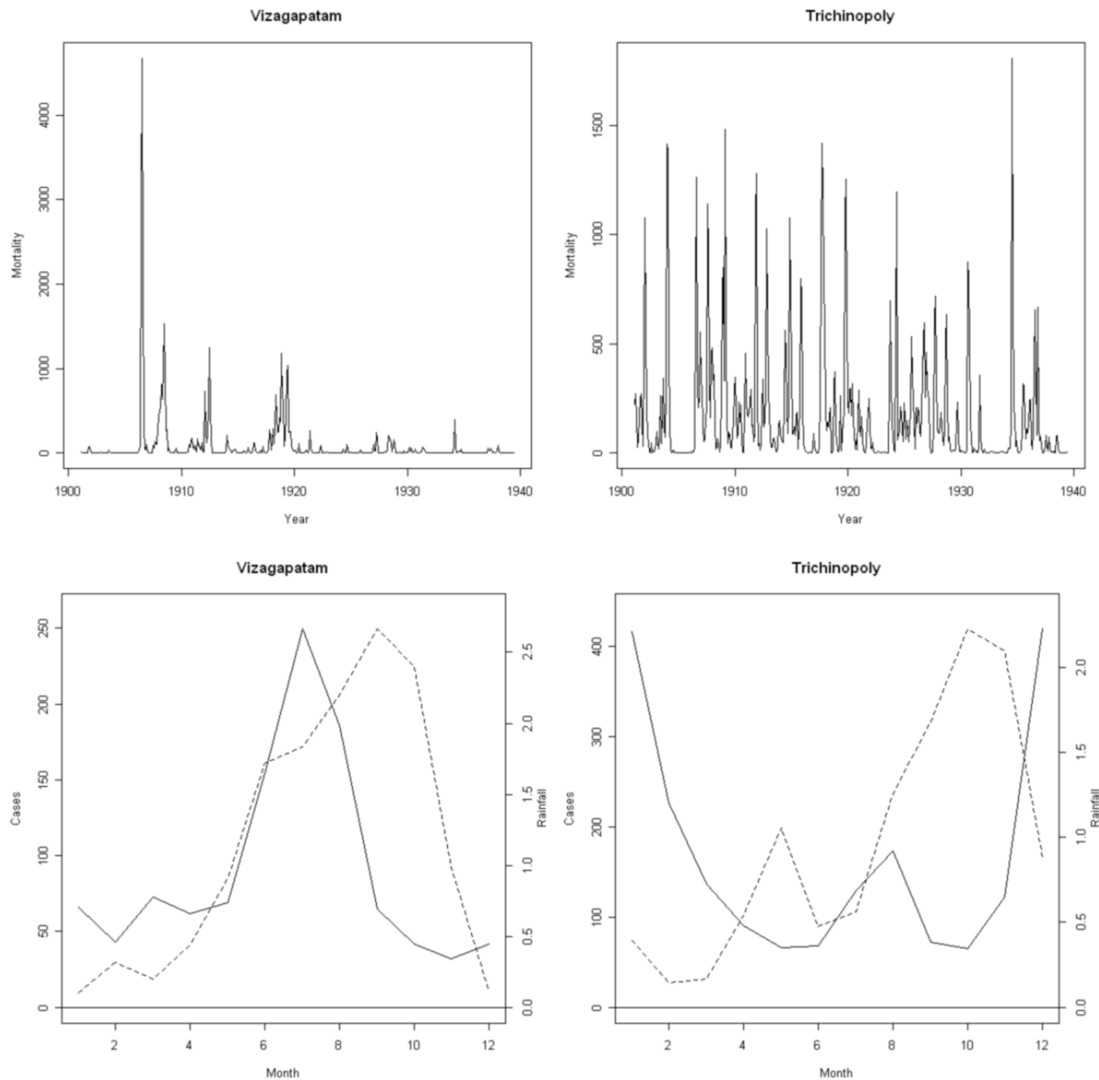


**Figure 2.3:** The upper panels show monthly cholera mortality from 1901 to 1940 for two representative districts for the two regions identified in this work: Vizagapatam (top, left) illustrates the intermittent epidemic patterns observed in the Northeast region; while Trichinopoly (top, right) exhibits the more regular seasonal pattern characteristic of endemic dynamics. The bottom panels show for these same districts, the monthly averages for rainfall (dotted lines) and cholera mortality (full lines) for these two districts. In Vizagapatam (bottom, left) one long rainy season typically coincides with cholera

outbreaks in years when disease is present; in Trichinopoly (bottom, right) two distinct rainy periods can be recognized that are typically out of phase with the two cholera mortality peaks.

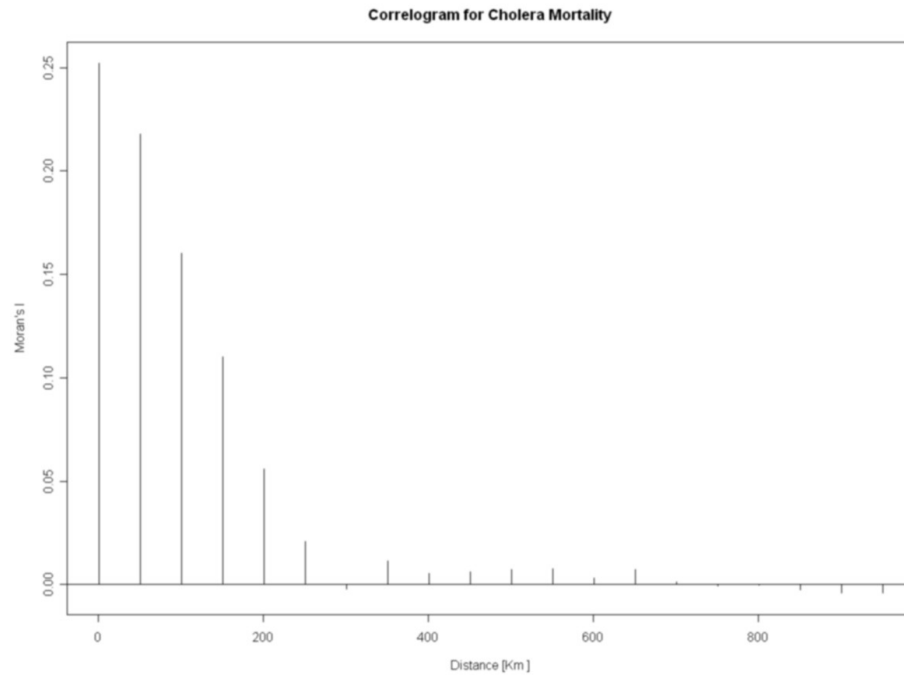


**Figure 2.4:** Spatial correlogram for cholera mortality in Madras computed from the mean value of cholera mortality per district and the distance between the districts' centroids. The value of the Moran's index indicates the influence of mortality across districts for a given distance. The distance of 200 Km. was selected as the boundary defining districts as "neighbors".

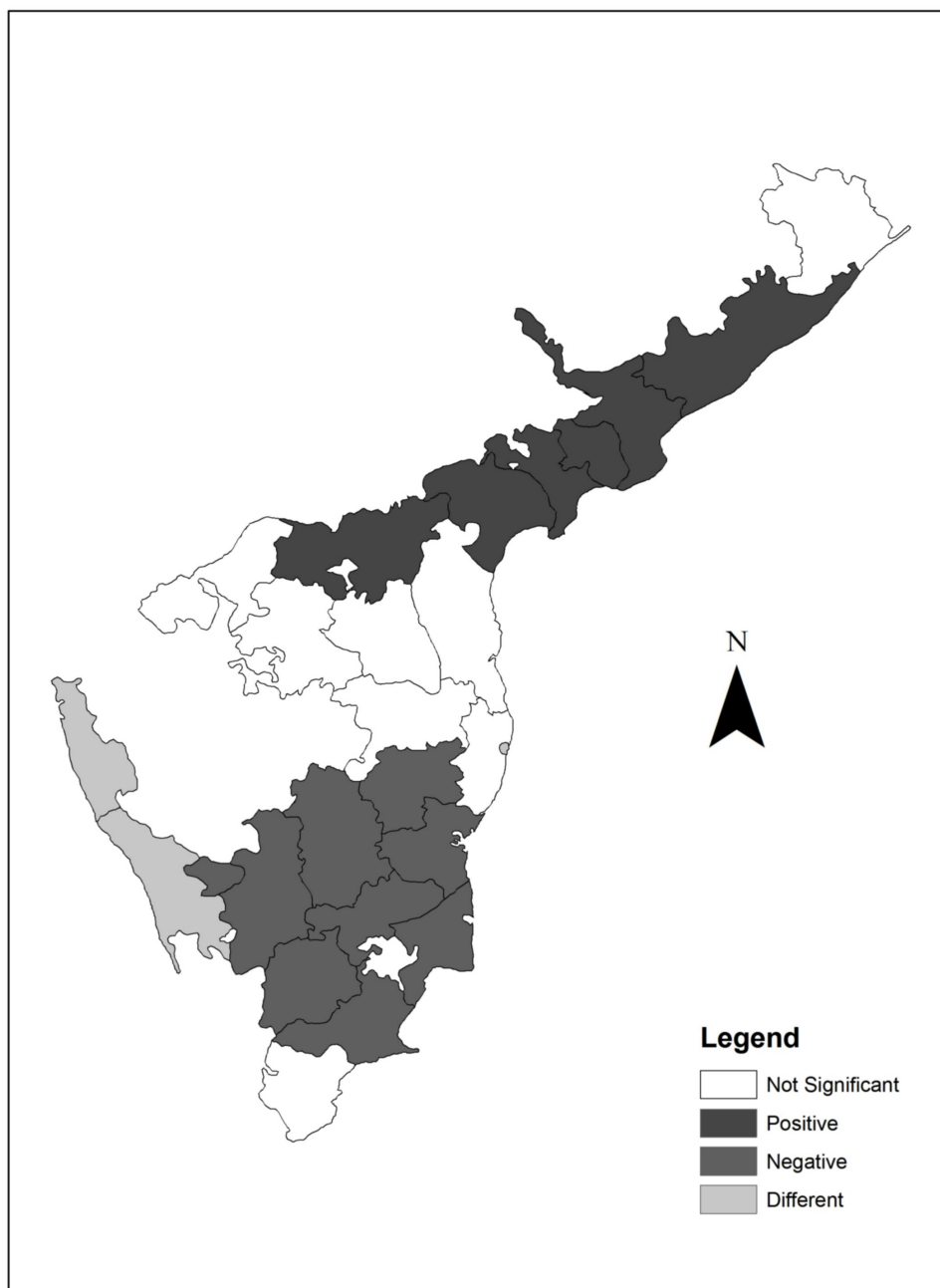


**Figure 2.5:** The LISA index applied to the coefficient of cross-correlation between cholera and rainfall (for zero lag). A cluster of positive correlation values between rainfall and cholera mortality is observed in the northeast region, while a cluster exhibiting negative correlation values is present in the south. Three districts show a statistically

different pattern from the districts defined as neighbors (presenting positive correlation values when their neighbors exhibit a negative value or vice versa). All clusters are statistically significant with  $p < 0.05$  for 999 random realizations.

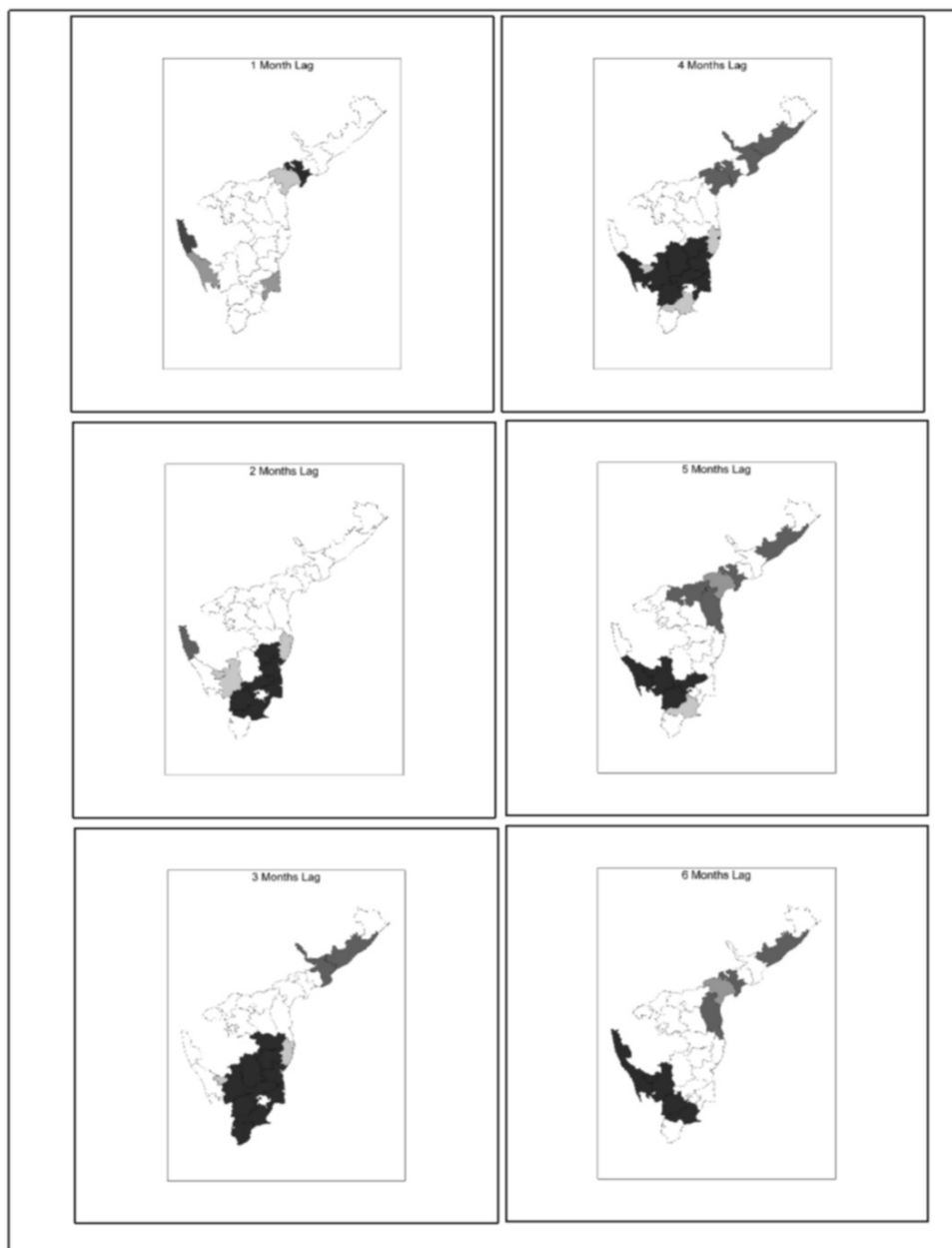


**Figure 2.6:** The LISA index applied to the coefficient of cross-correlation between cholera and rainfall for different time lags (with cholera behind rainfall). The color-coding is the same that the one described for Fig. 2.5. All clusters are statistically significant with  $p < 0.05$  for 999 random realizations.

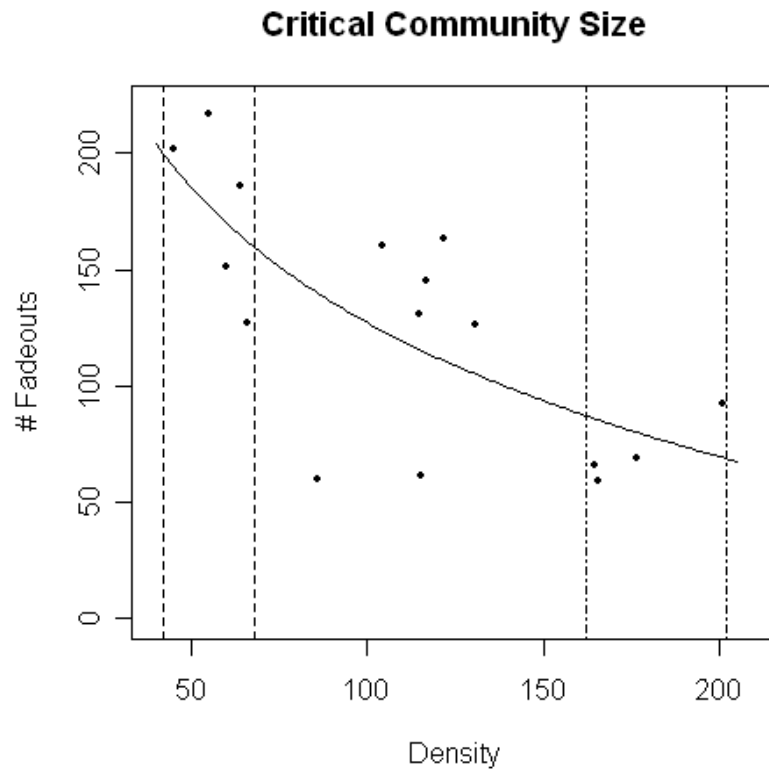


**Figure 2.7:** Critical Community Size, showing the number of fade-outs for the different districts against their population density [h/Km<sup>2</sup>]. The (logarithmic) fitted curve ( $R^2=0.5157$ ) illustrates the general decreasing trend in the number of fade-outs as density increases. The values obtained for the spatial autocorrelation, measured by the global index Moran's I, indicate that there is no significant spatial clustering neither for the number of fade-outs (Moran's I=0.14, p-value=0.08 for 999 random realizations) nor for the population density (Moran's I=0.17, p-value=0.06 for 999 random realizations). The low-density districts (between the vertical dashed lines on the left) exhibit irregular outbreaks, while those with higher population density (between the dot-dashed lines on the right) exhibit a regular seasonal pattern.

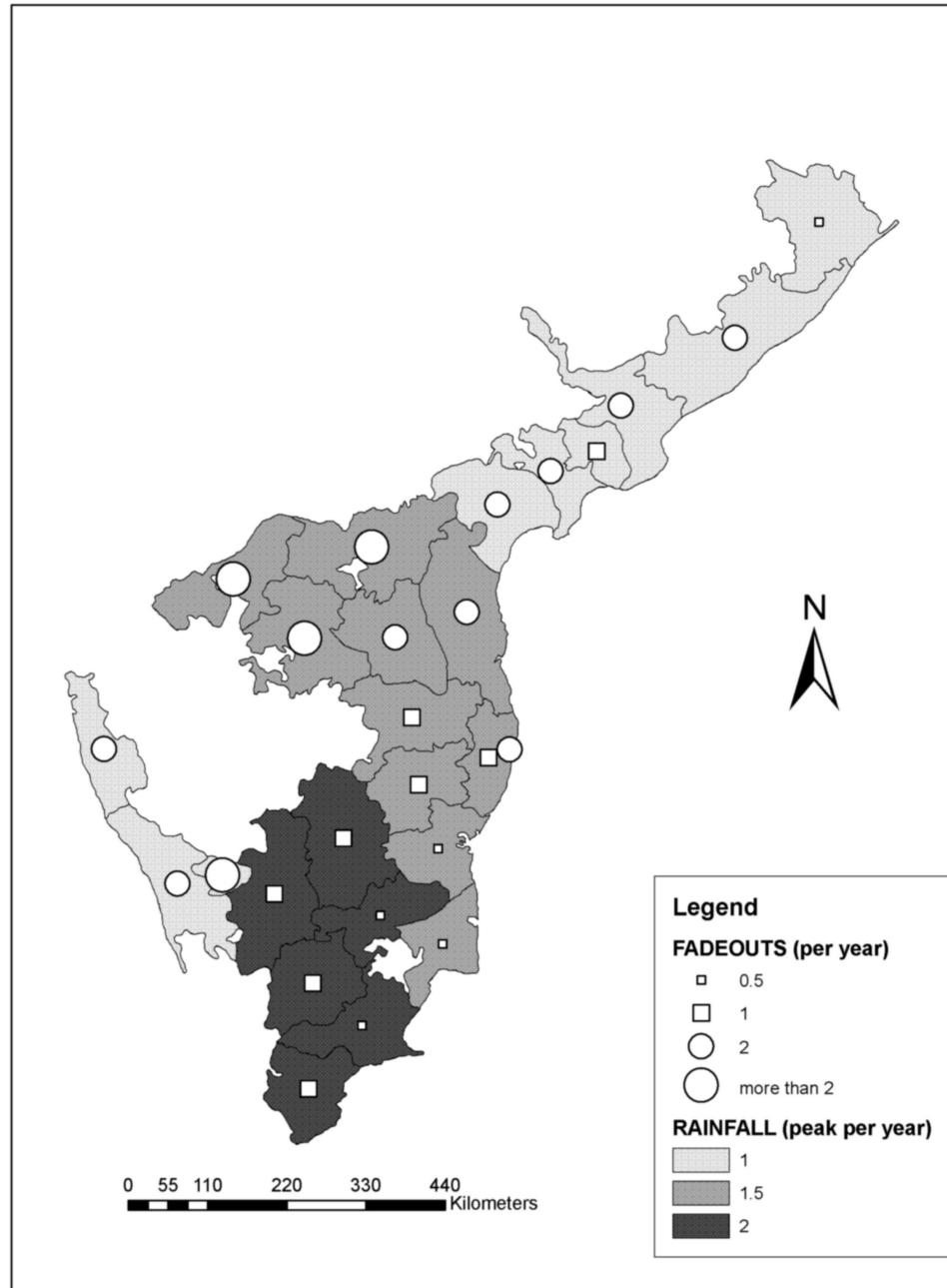


**Figure 2.8:** The spatial distribution of the average number of fade-outs and rainfall peaks per year. Districts with one and two peaks per year exhibit short and long rainy seasons respectively. The districts on the Arabian Sea (13, 15, and 20 in Fig.2) do not follow this pattern.



## References

1. Codeço CT: **Endemic and epidemic dynamics of cholera: the role of the aquatic reservoir.** *BMC Infectious Diseases* 2001, **1**:1—1.
2. Pascual M, Bouma MJ, Dobson AP: **Cholera and climate: revisiting the quantitative evidence.** *Microbes and Infection* 2002, **4**:237—245.
3. Koelle K, Pascual M: **Disentangling extrinsic from intrinsic factors in disease dynamics: A nonlinear time series approach with an application to cholera.** *American Naturalist* 2004, **163**:901—913.
4. Koelle K, Rodo X, Pascual M, Yunus M, Mostafa G: **Refractory periods and climate forcing in cholera dynamics.** *Nature* 2005, **436**:696—700.
5. Pascual M, Rodo X, Ellner SP, Colwell RR, Bouma MJ: **Cholera dynamics and El Niño-Southern Oscillation.** *Science* 2000, **289**:1766—1769.
6. Pascual M, Dobson AP: **Seasonal Patterns of Infectious Diseases.** *PLoS Medicine* 2005, **2**:e5.
7. Miller CJ, Feachem RG, Drasar BS: **Cholera Epidemiology in Developed and Developing Countries New Thoughts on Transmission, Seasonality, and Control.** *Lancet* 1985, **1**:261—263.
8. Kaper JB, Morris JG, Levine MM: **Cholera.** *Clinical Microbiology Reviews* 1995, **8**:48—86.
9. Colwell RR, Kaper JB, Joseph SW: **Vibrio Cholerae, Vibrio parahaemolyticus, and Other Vibrios: Occurrence and distribution in Chesapeake Bay.** *Science* 1977, **198**:394—396.
10. Colwell RR: **Global Climate and Infectious Disease: The Cholera Paradigm.** *Science* 1996, **274**:2025-2031.
11. Islam MS, Mahmuda S, Morshed MG, et al.: **Role of cyanobacteria in the persistence of Vibrio cholerae O139 in saline microcosms.** *Canadian Journal Of Microbiology* 2004, **50**:127—131.
12. Glass R, Claeson M, Blake P, Waldman R, Pierce N: **Cholera in Africa - Lessons on**

- transmission and control for Latin-America. *Lancet* 1991, **338**:791-795.
13. Merrell DS, Butler SM, Qadri F, et al.: **Host-induced epidemic spread of the cholera bacterium.** *Nature* 2002, **417**:642—645.
14. Hartley DM, Morris M, Smith DL: **Hyperinfectivity: A Critical Element in the Ability of *V. cholerae* to Cause Epidemics?** *PLoS Medicine* 2005, **3**:e7.
15. Pascual M, Koelle K, Dobson AP: **Hyperinfectivity in Cholera: A New Mechanism for an Old Epidemiological Model?** *PLoS Medicine* 2006, **3**:e280.
16. Faruque SM, Naser BI, Islam MJ, et al.: **Seasonal epidemics of cholera inversely correlate with the prevalence of environmental cholera phages.** *Proceedings Of The National Academy Of Sciences USA* 2005, **102**:1702—1707.
17. Bartlett MS: **Measles Periodicity and Community Size.** *Journal of the Royal Statistical Society. Series A (General)* 1957, **120**:48-70.
18. Keeling MJ: **Modelling the persistence of measles.** *Trends In Microbiology* 1997, **5**:513—518.
19. Bailey TC, Gratell AC: *Interactive Spatial Data Analysis.* Prentice Hall; 1985.
20. Fortin M, Dale MRT, ver Hoef J: **Spatial analysis in Ecology.** In *Encyclopedia of Environmetrics.* edited by El-Shaarawi AH, Piegorisch WW John Wiley & Sons, Ltd.; 2002, **4**:2051-2058.
21. Cliff AD, Ord JK: *Spatial autocorrelation.* London,: Pion; 1973:178.
22. Anselin L: **Local Indicators of Spatial Association LISA.** *Geographical Analysis* 1995, **27**:93–115.
23. Bjørnstad ON, Ims RA, Lambin X: **Spatial population dynamics: analyzing patterns and processes of population synchrony.** *Trends in Ecology and Evolution* 1999, **14**:427–432.
24. Bjørnstad ON, Stenseth NC, Saitoh T: **Synchrony and scaling in dynamics of voles and mice in northern Japan.** *Ecology* 1999, **80**:622–637.
25. Krishnamurthy V, Kinter III JL: **Global Climate .** In edited by Rodo X Spring-Verlag;

2002.

26. Bouma MJ, Pascual M: **Seasonal and interannual cycles of endemic cholera in Bengal 1891-1940 in relation to climate and geography.** *Hydrobiologia* 2001, **460**:147-156.

27. Koelle K, Pascual M, Yunus M: **Pathogen adaptation to seasonal forcing and climate change.** *Proc Biol Sci* 2005, **272**:971—977.

28. Lan RT, Reeves PR: **Pandemic spread of cholera: Genetic diversity and relationships within the seventh pandemic clone of *Vibrio cholerae* determined by amplified fragment length polymorphism.** *Journal of Clinical Microbiology* 2002, **40**:172–181.

## **Chapter 3.**

### **Spatial clustering in the spatio-temporal dynamics of endemic cholera**

#### **Background**

The spatial distribution of cases for infectious diseases that are environmentally driven, such as those of water-borne and vector-borne transmission, reflect the combined effect of environmental heterogeneity and disease dynamics. As such, spatial patterns can be used to examine hypotheses on routes of transmission at different scales [1-3]. For example, long-term disease data at the population level for multiple cities and towns, or presence-absence data in counties or districts, have provided numerous insights on patterns of propagation at the relatively large scales of countries and even transcontinental couplings [1, 4-6]. Detailed spatial records at the individual level have a long tradition at the interface of geography and epidemiology, with one of the best known examples found in the discovery of cholera's water source by Snow [7]. However, these detailed data have been typically short-term and limited to particular epidemics. Longer-term data sets at the high-resolution of individuals but spanning multiple epidemics are becoming available, with the current interest in transmission networks and the interface of Geographic Information Systems and disease patterns. This type of data makes possible the

description of how spatial patterns and clustering in particular, change in time, as a first step towards addressing the spatio-temporal dynamics of disease at a high resolution, as well as the coarse-graining of these dynamics, from small, individual, to large, population, levels.

In general, higher case numbers are expected in areas surrounding pathogen sources, and lower ones, in areas far away from these sources. For example, for vector-borne diseases, the clustering of cases might occur nearby the specific habitat of the vector, and for water-borne diseases, in the proximity of infected aquatic reservoirs. However, patterns are complicated by the fact that transmission can occur from both environmental reservoirs and previously infected individuals, reflecting the dynamics of transmission, human behavior and environmental variability. For cholera, an acute diarrheal infectious disease caused by the bacterium *Vibrio cholerae*, two routes of transmission have been proposed [8], the first one from aquatic reservoirs in the environment, and the second one, from previously infected individuals. To address the respective roles of these two routes of transmission, this paper examines the clustering patterns of cholera and how they vary in time with an extensive data set for a rural area of Bangladesh, covering twenty years and groups of households in the landscape.

Although the cholera bacterium has an enormous diversity with more than 200 serogroups classified based on the somatic O antigen, only two such groups, O1 and O139, are pathogenic [9-11]. *V. cholerae* O1 can be subdivided in turn into two biotypes (phenotypes), classical and El Tor [12]. The O1 serogroup can also be subdivided into

serotypes (based on antigenic responses) called Ogawa, Inaba and the extremely rare Hikojima [11]. Moreover, the Bengal strain, *V. cholerae* O139, appeared in 1992 [13] presumably by horizontal gene transfer between O1 and another O serogroup [11]. Nowadays, evidence from field studies and epidemiological models, supports the fact that the classical variant is more infective than the El Tor variant. However, the El Tor variant is more resilient outside the human host, surviving in the environment for a longer period than the classical strain [14, 15]. Recent evidence suggests that *V. cholerae* O139 performs better in both, the environment and the human gastrointestinal tract [16], raising questions on its short epidemic period.

Survivorship of the pathogens, availability of susceptible individuals and temporal immunity appear to be important processes shaping the pronounced seasonality of cholera. In non-endemic locations (like Peru, Brazil and several countries in Africa), epidemics are confined to the warm and rainy season. By contrast, in endemic areas in Bangladesh and former Bengal, two epidemic peaks occur each year corresponding to the warm seasons before and after the monsoonal rains [10, 17]. A full explanation of this complex seasonal pattern is still lacking, and a number of environmental and ecological drivers have been proposed (for example, the presence of environmental cholera phages, the degree of crowdedness and availability of susceptible individuals) [18]. For estuarine regions of Bangladesh with two peaks per year, evidence supports a relationship between the initiation of the spring peak of cholera and favorable environmental conditions for the bacterial population, such as warmer temperatures [19]. A dilution effect would then

drive the reduction of cholera during the monsoonal season [17], although recent mathematical models of historical mortality time series, suggest an alternative explanation in which susceptibles are depleted by a large number of asymptomatics and short-term immunity [20]. Finally, an increase in human-to-human contact, as a consequence of the post monsoonal floods might be an important factor in the second epidemic peak [21].

Infectivity and survivorship affects the spatial distribution of *V. cholerae* and its availability to colonize susceptible individuals. From this perspective, an initial study on the spatial occurrence of cholera cases by Glass and colleagues [22] provided a detailed description of cholera epidemics during the period from 1966 to 1980. This study identified villages with high and low cholera risk. Based on these findings, Miller and colleagues proposed a cholera model with two routes of transmission, primary and secondary, respectively [23]. Primary transmission occurs as the result of eating contaminated shellfish or aquatic plants, and drinking contaminated water. Secondary transmission results instead from a 'person-to-person' infection. Thus, primary transmitted cases should be scattered in space, occurring almost simultaneously in different areas with no apparent interconnection, and should be located relatively close to water sources. These initial cases would be followed by the clustering of secondary transmitted cases [23] Miller and colleagues further proposed that primary transmission shapes the seasonal patterns in endemic areas, whereas secondary transmission determines the level of infection.

It is important to note that secondary transmission can occur directly or indirectly (i.e., via fecally contaminated water), and that it can involve the same aquatic reservoirs than those of primary transmission. These two modes of transmission effectively represent the two extremes of a possible continuum, with the key distinction being the degree of memory in the current force of infection of previous levels of infection. Only the secondary route possesses this memory, and this is the sense in which ‘human-to-human’ transmission should be interpreted.

The study of spatial cholera patterns by Craig further addressed the existence of clustering with case data from 1970 to 1982 at the level of baris, patrilineally related household groups [24]. A significant excess of cases was detected at short distances, “within baris” of less than 250 m, and short time intervals (3 and 10 days). However, this analysis did not take into account that the spatial location of cases is not random and that the distribution of the baris themselves must be taken into account. It also did not consider the timing between the occurrence of clusters and the epidemic peaks, and the nature of the clustering (positive or negative). Nevertheless, Craig’s study was the first description of cholera’s spatial distribution in an endemic area at high resolution.

We further examine here the spatio-temporal distribution of cholera cases in Matlab, Bangladesh, to address the occurrence of clustering during epidemic years. We specifically consider the relationships between cluster size and epidemic intensity, between the timing of clustering and the epidemic curve, and that between clusters of cases and water sources. Primary transmission from water reservoirs is believed to occur



when environmental conditions are favorable [19, 25]. A spatial association between cholera cases and water sources should be observed if primary transmission drives the development of epidemics, with no significant spatial correlation between observed cholera cases at the beginning of the outbreak [8]. Because water sources (rivers, canals and water ponds of diverse size) are found almost everywhere and are extremely abundant in our study area, they are not likely however to impose significant spatial constraints on the occurrence of cases. Thus, cases generated by environmental transmission should occur almost anywhere. By contrast, once epidemics have reached a threshold size, secondary transmission should dominate the dynamics, generating spatial associations between cases. This pattern should be, most pronounced during the fall peak after the monsoonal rains, when secondary transmission has been suggested to play a more important role [17, 21], since flooding disrupts sanitary conditions and concentrates human populations in the landscape. This hypothesis would predict a significant clustering of cases during the fall peak and a weak spatial association between cholera cases and water sources. We examine these predictions here.

### **Methods and Data**

The data for this study come from the rural area of Bangladesh known as Matlab, located about 50 km south-east of Dhaka, the capital of the country. The study area is adjacent to the confluence of the Meghna and the Ganges Rivers, and is bisected by the Dhonagoda River into two approximately equal parts. Numerous canals and water ponds

are present in the whole region (Fig. 3.1).

People in this area live in groups of patrilineally related households known as *baris*, with an average of six households [26]. Starting in 1994, a spatial database was created to facilitate the analysis of health and population research. All the *baris* were identified by a census number by the ICDDR (International Centre for Diarrhoeal Disease Research, Bangladesh) demographic surveillance system, allowing incidence data to be linked to the specific location of a single *bari* [26, 27]. Complementing the information on *baris*, geographic coordinates of major water sources (i.e. big water ponds) were also acquired. Surface untreated water from ponds and rivers is used for villagers not only as drinking water but also for other household uses [28], since water from tube wells has been found to be contaminated with arsenic. Our analyses focus on the cholera cases from 1983 to 2004 for 8340 *baris* of this spatial database.

Health data were obtained from both surveillance and laboratory analyses. Individual health and demographic surveillance data were regularly collected for all individuals living in the Matlab study area. The Matlab hospital is the only diarrheal treatment center in the rural area, providing free treatment to all patients. Stool samples for all patients were collected and screened for enteric pathogens in the laboratory. Cholera cases were registered using the date of admission to the hospital and both biotype and serotype were reported.

During the study period, 7241 cholera cases were recorded (1972 cases correspond to classical O1 and 5269 cases, to El Tor O1). Temporal variability is evident at both

seasonal and inter-annual scales in the data (Fig. 3.2). The spatio-temporal information for all cases was used to analyze the spatial clustering of cholera cases per sé (clustering of cases from now on), the spatial clustering of cholera cases with respect to the available water sources locations (clustering of cases-water from now on) and the timing between the occurrence of significant spatial associations and the dynamics of the epidemics.

The clustering of cases was studied using spatial statistics derived from the popular Ripley's K index [2, 29]. The Ripley's K index quantifies nonrandom clustering patterns (by estimating the second order effects from an observed point pattern). For a particular region  $\mathcal{R}$  with area  $R$ , where  $n$  events (i.e. infections) have been observed, the Ripley's K index can be estimated as:

$$\hat{K}(h) = \frac{R}{n^2} \sum_{i \neq j} \frac{I_h(d_{ij})}{w_{ij}} \quad (3.1)$$

where the function  $I_h(d_{ij})$  indicates whether or not the events  $i$  and  $j$  occurred within a distance less than or equal to  $h$ ; and  $w_{ij}$  is an edge correction to handle arbitrary shaped regions [29, 30]. It is important to notice that the K function considers the intensity, the mean number of events (infections) per unit area, of the process under analysis, and therefore the detection of a clustered distribution means that the number of cases (more properly, events) is above the expected density of cases at that particular scale.

The K function can be easily transformed into the well-known L function, estimated by:

$$\hat{L}(h) = \sqrt{\frac{\hat{K}(h)}{\pi}} - h \quad (3.2)$$

When  $\hat{L}(h)$  is plotted against  $h$ , the peaks for positive values indicate spatial attraction of events, or clustering, whereas the troughs for negative values indicate the spatial repulsion, or regularity, at the corresponding scale of distance  $h$  in each case. Zero values indicate a random spatial distribution. Ripley's K and L functions were calculated by aggregating the daily cholera data into temporal windows ranging from 2 to 17 days. This allowed the inclusion of sufficient cases to statistically evaluate clustering for most strains, except for El Tor O1 Ogawa whose epidemics were too sparse to be considered in these analyses.

Two important factors must be considered in the spatial analysis of cholera cases. First, their spatial location is constrained by the spatial location of baris. Second, the baris themselves are not homogeneously distributed in the Matlab region. One way to take into account these deviations from the original tests, is to perform Monte Carlo replications for the sequence of cholera cases over time, and thus evaluate significance accounting for the underlying landscape. Spatial clustering and repulsion are statistically significant when the observed L values are outside the envelope defined by the maxima and minima of the Monte Carlo replications (technical details in Fig. 3.3). The spatial distances for which the Ripley's functions were calculated (the maximum value for  $h$  in formulas (3.1) and (3.2)) were restricted to below 8 kilometers because of the size of the study area (which spans approximately 18 kilometers in longitude and 22 kilometers in latitude).

The spatial clustering and/or repulsion of cases-water was studied by using a cross

K function. For this analysis, cholera cases and water sources are considered as two different types of events (rivers and canals were not included in this analysis). Under the assumption of independence between types of events, the location of one type should be random with respect to that of the other type, regardless of the overall spatial distribution of either type. Hence if cases originated from water sources, the location of cases will be correlated with the location of water sources, and therefore the K function will identify such relationship as clustering at particular scales. Following the previous reasoning, the L function can be used to consider the interaction of two (or more) types of events, to evaluate spatial attraction, independence or repulsion (see [29] chapter 4 for details). An equivalent bootstrapping technique was used to evaluate the statistical significance of the clustering of cases-water.

For both spatial analyses (clustering of cases and cases-water), the characteristic cluster size was defined as the distance corresponding to the largest significant difference (i.e. the most significant difference). Hence, the largest difference between the observed L values and the corresponding superior envelop from the bootstrapping was considered as the characteristic cluster size [29]. Note that during the course of an epidemic, significant clusters may occur at several scales (Fig. 3.3), but only the most significant is considered for the analyses presented in this work.

During the study period, several cholera outbreaks with different intensity occurred. To reduce the variability presented in the data we defined (and analyzed) epidemics as outbreaks that surpassed 30 new cases during the course of a week. This is

based on the observed distribution of epidemic sizes. Although epidemics exhibited the typical seasonal pattern of two peaks per year during most of the study period, the timing of initiation of these peaks exhibited variability from year to year. Based on the ideas from Cazelles and Stone [31], we rescaled time for each epidemic as follows: Each epidemic was mapped onto the interval  $[0, \xi\pi]$ , with the beginning mapped to time 0, the first (fall) peak to  $\pi$ , the inter-peak decay to  $\nu\pi$ , the second (spring) peak to  $\nu\pi$  and finally the end of the epidemic to  $\xi\pi$ . Four stages (1 to 4) were thus defined, with stages 1 and 3 corresponding to the rise of epidemics (fall and spring), and stages 2 and 4, to their decay.

## Results

During the period of study, cholera epidemics in Matlab exhibited the typical pattern of two peaks per year (Fig. 3.4) reported for other endemic areas in Bangladesh [17] and some areas in historical Madras [21]. This pattern was observed regardless of the specific strain (Fig. 3.2). Moreover, the fall peak (corresponding to  $\pi$  in the figures) is bigger than the spring peak (in Fig. 3.4, Kruskal-Wallis test  $\chi^2=21.5255$ ,  $df=1$ ,  $p$ -value= $3.492e-06$ , for a temporal aggregation of 7 days, see Table 3.S1 in the supplemental material for other examples). The decay of cholera cases during the monsoon season usually leads to a fade-out of the epidemic, while the decrease in the winter rarely reaches extinction.

We present representative results based on the (most significant) cluster size for

cholera cases (see Methods), however it must be noticed that high variability is present in both data (Fig. 3.2) and results (Fig. 3.5). All yearly epidemics display several significant clusters of cases with varying sizes. Moreover, cluster sizes fall into two dominant scales, a small spatial scale (hundreds of meters) and a relatively large scale (ranging from 3 to 6 Kilometers), bigger clusters are rare (Fig. 3.5a). These spatial scales are present independently from the temporal scale of aggregation of the cases (see supplemental material). In addition, significant clusters are not present in a continuous way (i.e. a random pattern is detected at several intermediate scales, Fig. 3.3 and Fig. 3.5a). Finally, the most significant cluster size exhibits high variability during the course of epidemics, but big cluster sizes correspond to peaks in epidemic size.

A less clear pattern is obtained for the clusters sizes corresponding to cases-water (Fig. 3.5b). Clusters of different sizes are present at different times, although few clusters seem to be present during the winter (corresponding to  $\forall \pi$  in Fig. 3.5b).

Results for the dynamics of clustering are summarized in Figure 3.6 where the dynamics of epidemic size and cluster size (for cases and cases-water) averaged over all epidemics for each particular strain are shown. No surprisingly, cluster size tracks epidemic size. Sudden changes in epidemic size are reflected in either cluster size of cases and/or cases-water sources. A closer look reveals some additional features. The size of the clustering of cases-water sources is, in general, bigger than that corresponding to clustering of cases. As expected significant clustering appears with some delay with respect to the onset of the epidemics (for both peaks) (see also Fig. 3.5). Clusters occur

more frequently during the decay than during the onset of the epidemics (regardless of the peak), and also are more frequent during the fall than during the spring peak (regardless of the rate of increase of epidemics) (see Tables 3.1 and 3.2).

The distribution of cluster sizes exhibited by the different strains (over all epidemics) is shown in Figure 3.7. The first row show the distribution of cluster sizes for cases and the second row, for cases-water. For classical Ogawa epidemics (Fig. 3.7 top-left) the distribution of cluster sizes for cases displays two characteristic sizes (around 200 m. and 5000 m.). The distribution of cluster sizes for cases-water on the other hand shows one typical scale around 7100 m. (Fig. 3.7 bottom-left). For classical Inaba epidemics (Fig. 3.7 top-center) the distribution of cluster sizes for cases displays also two characteristic sizes (around 200 m. and 4000 m.), but the distribution of cluster sizes for cases-water does not exhibit a characteristic scale (Fig. 3.7 bottom-center). The distribution of cluster sizes for cases of El Tor Inaba (Fig. 3.7 top-right) shows a small characteristic scale (150 m.), however two characteristic scales are found in the distribution of cluster sizes for cases-water (around 800 m. and 7000 m.).

## **Discussion**

Our results indicate that primary transmission sparks the start of epidemics at several distant locations more or less synchronously. This generates the clustering of cases only at big scales with respect to water sources, as opposed to small clusters close to a few punctual sources. Secondary transmission follows, and the clustering of cases at



relatively small scales becomes dominant. At the larger scales, however, these new cases create a relatively homogeneous spatial distribution because of the multiple origins of seasonal outbreaks, and therefore clustering with respect to water sources persists for those scales most of the time. The onset of epidemics is therefore controlled by both secondary and primary transmission. However, rapid increases in the number of cases are clearly tracked by spikes in clustering, indicating that secondary transmission plays a fundamental role in the development of epidemics. These findings are consistent with the interpretation of cholera patterns previously proposed by Miller and colleagues [23].

Additional support for the fundamental role of secondary transmission during the onset of the epidemics is provided by the fact that the “epicenter” of the epidemic (calculated as the center of mass for the location of cases) moves during the course of the outbreaks (results not shown). A more constant epicenter would reflect the spread of epidemics from an initial source of contamination.

Spatial clustering practically disappears during inter-epidemic periods, as expected, with a few randomly spatially distributed cases (if any) occurring until the beginning of another outbreak (Fig. 3.5 and Fig. 3.6). The spatial clustering of cases is detected at several scales, with two dominant sizes, given by hundreds of meters and a few kilometers, consistent across the different epidemics. These two scales suggest the occurrence of long distance transmission events that might be triggered (among other causes) by the movement of asymptomatic individuals, given their importance during epidemics [20].

The frequency of cluster occurrence (Tables 3.1 and 3.2) showed that the clustering of cases-water occurs more often than that of cases. This difference is consistent with the observation of cases-water clustering from the very beginning of outbreaks as primary transmission triggers epidemics. It is also consistent with the clustering of cases emerging with some delay but still in the early stages of epidemics, as secondary transmission becomes established and dominates the dynamics (Fig. 3.5 and Fig. 3.6). This pattern exhibits small differences among the different strains. The contamination by secondary cases of new water sources could explain the persistence of clustering at large scales for cases-water.

The spatial clustering pattern observed during the decay of the outbreaks is sometimes indistinguishable from a random spatial pattern (Fig. 3.5 and Fig. 3.6). This could be due to several factors. One possibility is that, the increase in rainfall and associated dilution effect, might eliminate the spatial structure. In addition, heterogeneity in the recovery time of infected individuals and behavioral changes, induced by the presence of cases, would alter the observed spatial pattern. This random pattern could also reflect a failure of the chain of transmission of the disease, with the re-initiation of epidemics from environmental sources.

The lack of strong seasonality on the presence of cases-water clustering (Table 3.2) could reflect the effectiveness of water sources as a reservoir and their role as a 'link' between the clusters of secondary cases. Some of the variability in the effectiveness of water sources might result from strong ENSO events which have been shown to be

strongly associated with cholera epidemics [32].

Finally, the analyses presented in this work are based on a static framework, where clustering is calculated from snapshots. A natural next step is to incorporate dynamical feedbacks between disease processes and the state of the population together with seasonality. Stochastic spatio-temporal models, similar to the ones developed for the advance of the “epidemic front” for rabies in the USA [3, 33], are under construction. The rabies model identified in particular the consequences of spatial heterogeneity for the spread of the front of infection. Endemic dynamics such as those of cholera in Bangladesh require the development of stochastic models that not only describe the propagation of a front but are also able to include the “back-propagation” to areas with both previously uninfected (still susceptible) and/or recovered individuals. Nested models can be formulated to evaluate the role of primary and secondary transmission, as well as the importance of immunity and cross-immunity in determining the complex spatial patterns observed in cholera dynamics [34, 35]. This work would extend the current scope of metapopulation and individual-based models of infectious diseases, to consider the stochastic dynamics that arise at high spatial resolution for diseases with temporary immunity. Such high resolution models would provide a basis to examine how to scale the dynamics up to the population level, to the simpler temporal models that are currently used for cholera and other infectious diseases in confronting time series data (e.g. [1, 3, 4, 20, 36, 37, 33, 38-43]). These approaches will lead to a better understanding of the importance of spatial structure in the temporal dynamics of the disease.

**Table 3.1: Presence of significant clustering for cases.** Proportion of time that significant clustering was exhibited (corrected for the presence of the disease) for clusters between cases.

		Proportion of time with sig. clustering of cases		
	Interval	classical Ogawa	classical Inaba	El Tor Inaba
Fall Peak	$[0 - \pi]$	0.7277778	0.9217877	0.9722222
	$[\pi - 2\pi]$	0.821839	0.8888889	0.9611111
Spring Peak	$[2\pi - 3\pi]$	0.6258503	0.9277778	0.8833333
	$[3\pi - 4\pi]$	0.7205882	0.8111111	0.97

**Table 3.2: Presence of significant clustering for cases-water** Analogous to Table 1, but considering the clustering of cases with respect to water sources.

		Proportion of time with sig. clustering of cases-water		
	Interval	classical Ogawa	classical Inaba	El Tor Inaba
Fall Peak	$[0 - \pi]$	0.8	0.9664804	0.999435
	$[\pi - 2\pi]$	0.8850575	0.9991245	0.99964
Spring Peak	$[2\pi - 3\pi]$	0.7142857	0.9833333	0.97
	$[3\pi - 4\pi]$	0.867647	0.8666667	0.999187



**Figure 3.1: Study Area.** The Matlab rural area. Light gray points are mapped water sources (ponds), dark gray points are baris and, as example, black points map cases from one epidemic of cholera classical Ogawa. Black lines represent the limits of the study area and light gray lines are rivers.

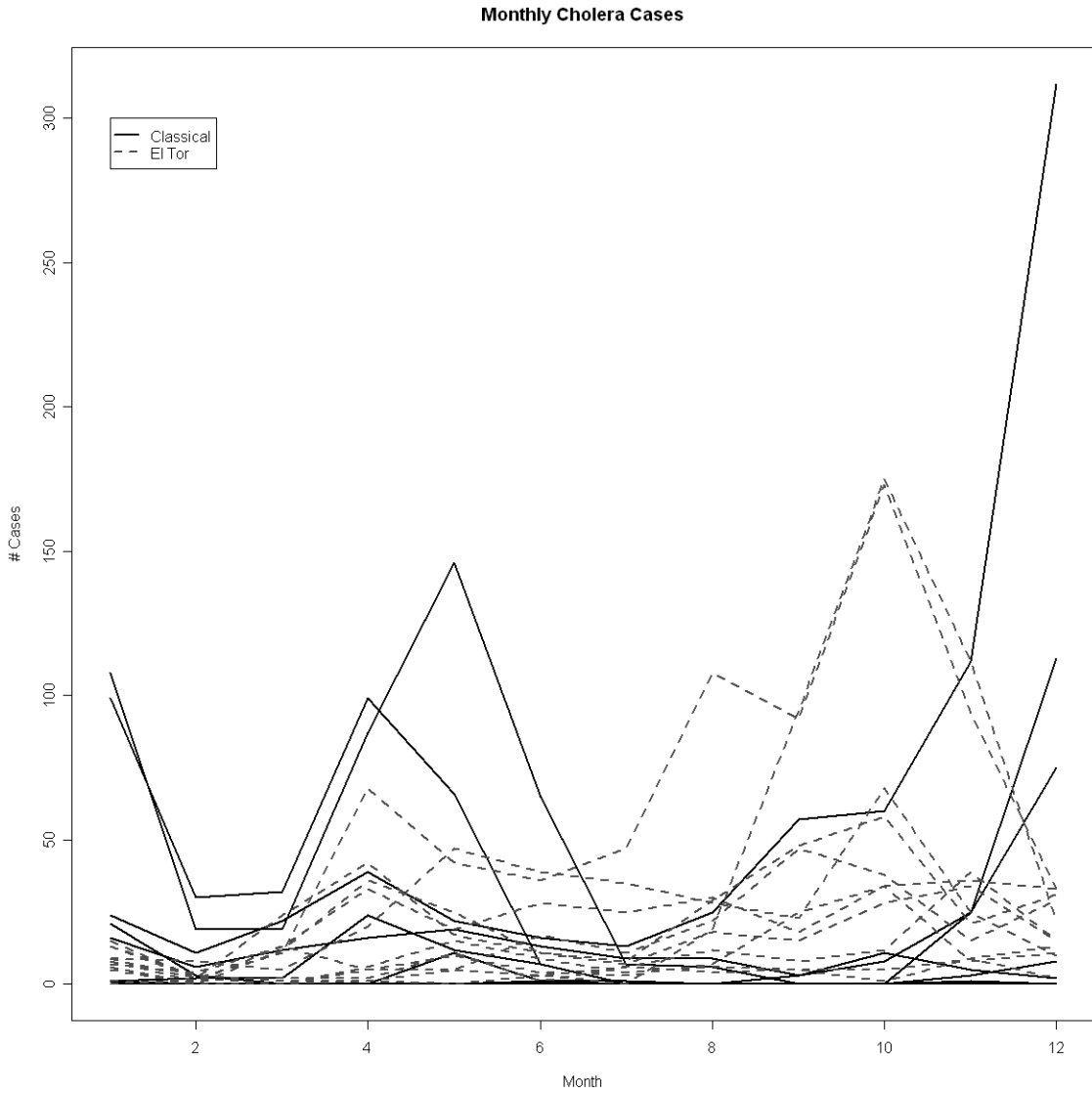


**Figure 3.2: Temporal Dynamics of Cholera epidemics.** The different lines represent annual cholera epidemics, solid black lines correspond to epidemics of classical (Inaba and Ogawa) strain, dashed dark gray lines show El Tor epidemics (Inaba and Ogawa). Variability is strongly marked, not only inter-annual or seasonality, but also intra-annual variability in both the timing of the outbursts and magnitude of the epidemics.

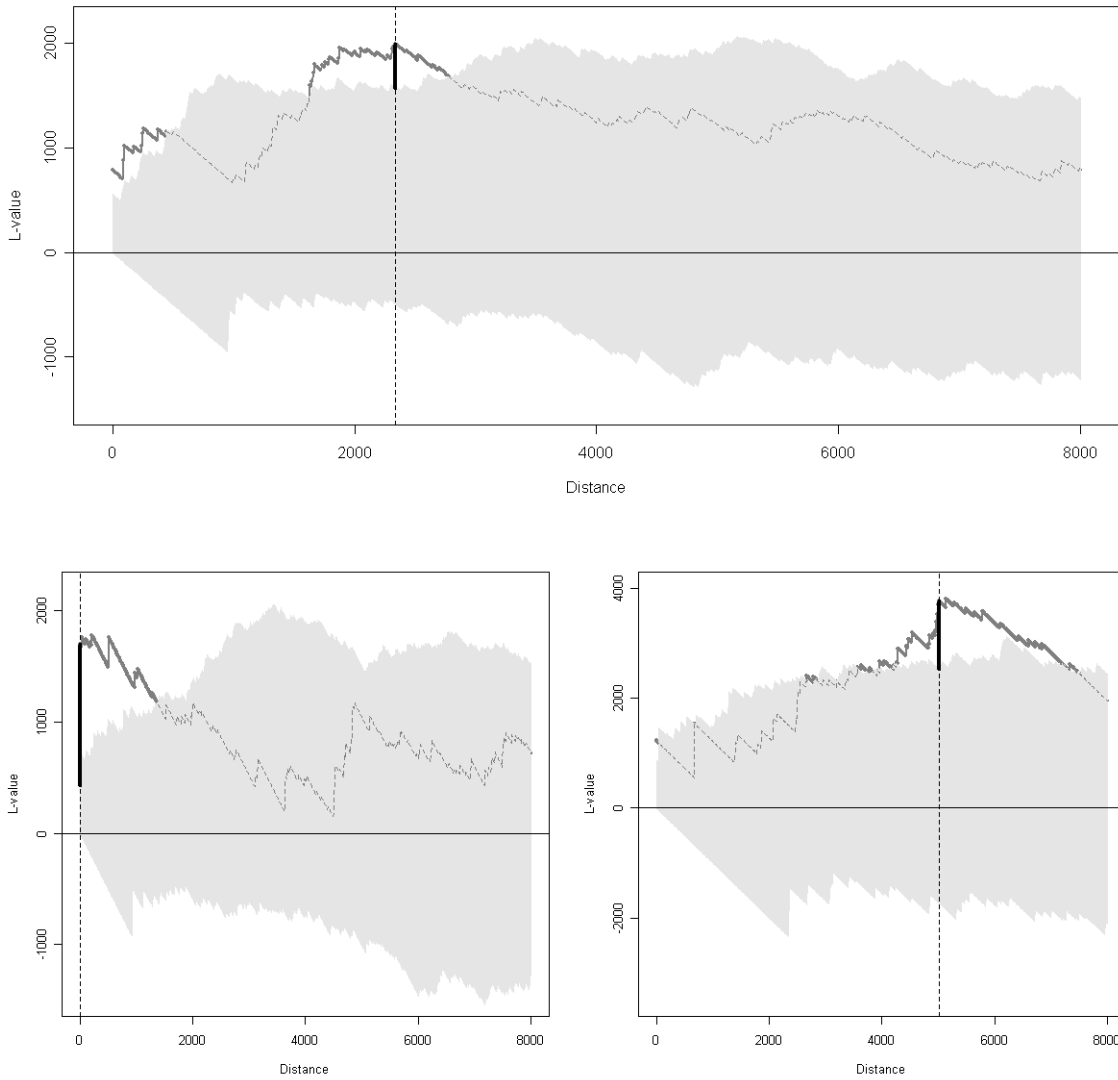


**Figure 3.3: Ripley's L function for a particular epidemic.** These three examples show variability and characteristics of the spatial clustering. Plotted in dark gray, the Ripley's L function for the observed data against distance. The Ripley's L function for observed data (dark gray) is plotted bold when statistically significant (i.e. outside the bootstrapping envelop), but otherwise is dashed. The light gray area was defined by the 10000 bootstrapping replications, these replications were constructed using all the cases for a

particular epidemic. The most significant cluster size, or simply cluster size, is defined as the distance at which the difference between the bootstrapping envelope and the observation is maximum (black bold vertical segment), this is indicated by the vertical dashed line in the figure. The top panel shows a case where the cluster size is relatively large (2340 meters) but small-scale significant clusters are also present. The bottom-left shows a cluster size with small scale (50 meters) without the occurrence of clusters at large scales. The bottom-right displays a large cluster size (5010 meters) without clusters at small scales.



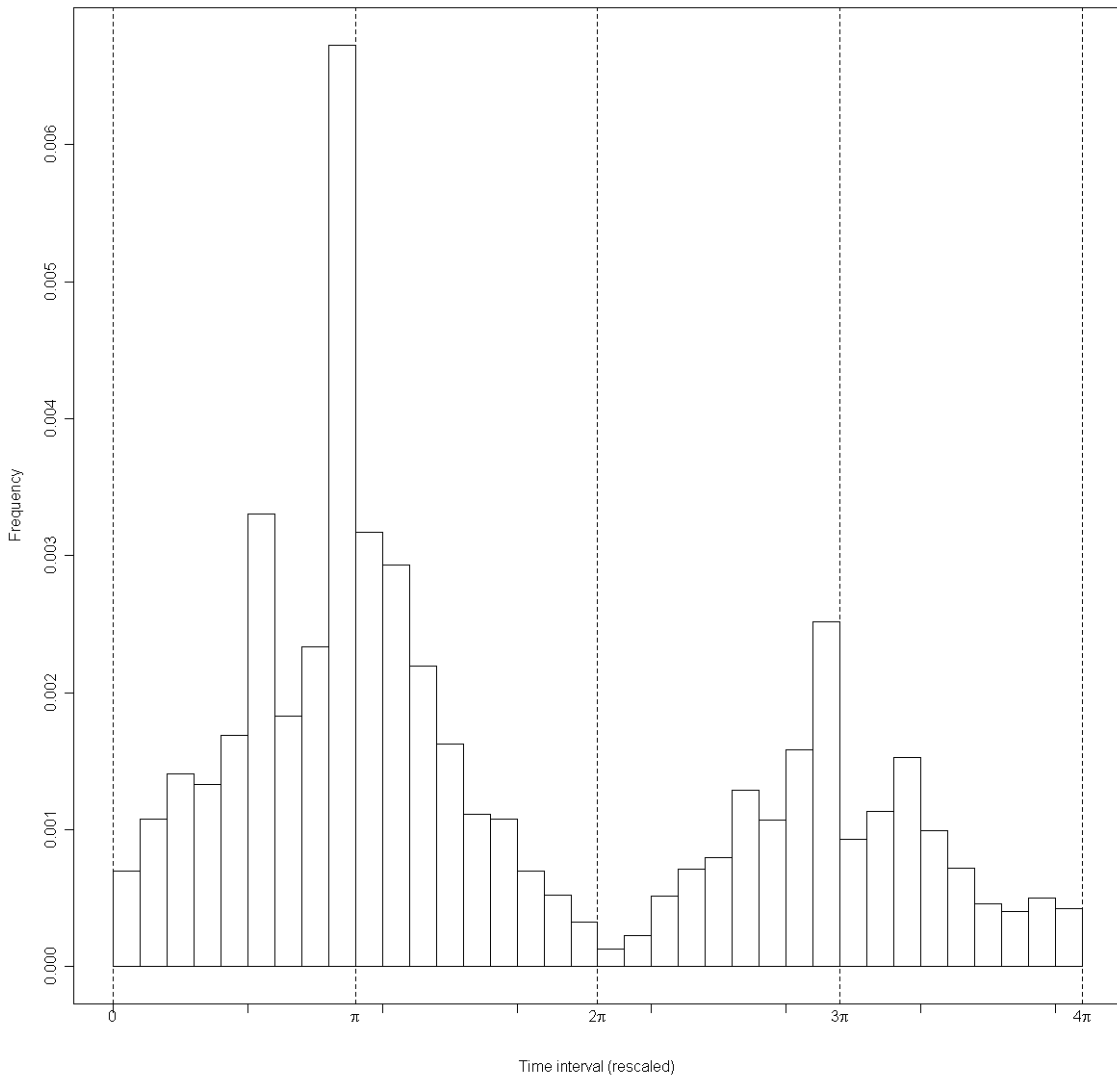


**Figure 3.4: Cholera seasonality.** Seasonal variation is shown on the mean number of cholera cases (El Tor Inaba) during the epidemics. In this plot, the time has been rescaled and hence outbreaks from several years were aggregated. The vertical lines show beginning, first peak, the inter-epidemic trough, second peak and end of the average occurrence of cases.

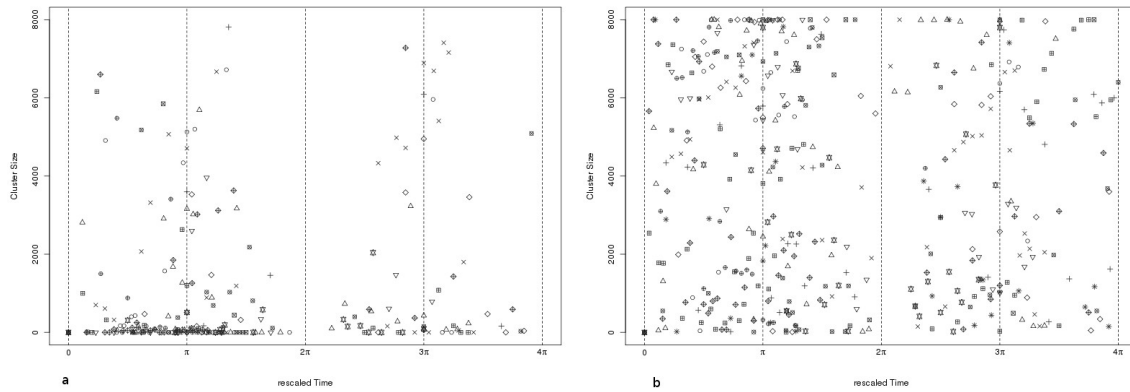


**Figure 3.5: Cluster size for the different epidemics.** Time has been rescaled,  $\pi$  represents the fall peak and  $3\pi$  the spring peak. Cluster Size for cases is shown in (a) and cluster size for cases-water in (b) Different symbols represent different epidemics a temporal window of 5 days for the disease data was used for this figure, but see additional figures for a disaggregation for the different epidemics and temporal windows. In (a) the occurrence of small clusters is clearly abundant, moreover, medium size clusters (less than 6 Km) are less abundant and bigger clusters are rare, this pattern is not clear for (b). In addition, clusters clearly occur more often in the fall peak an in the spring.

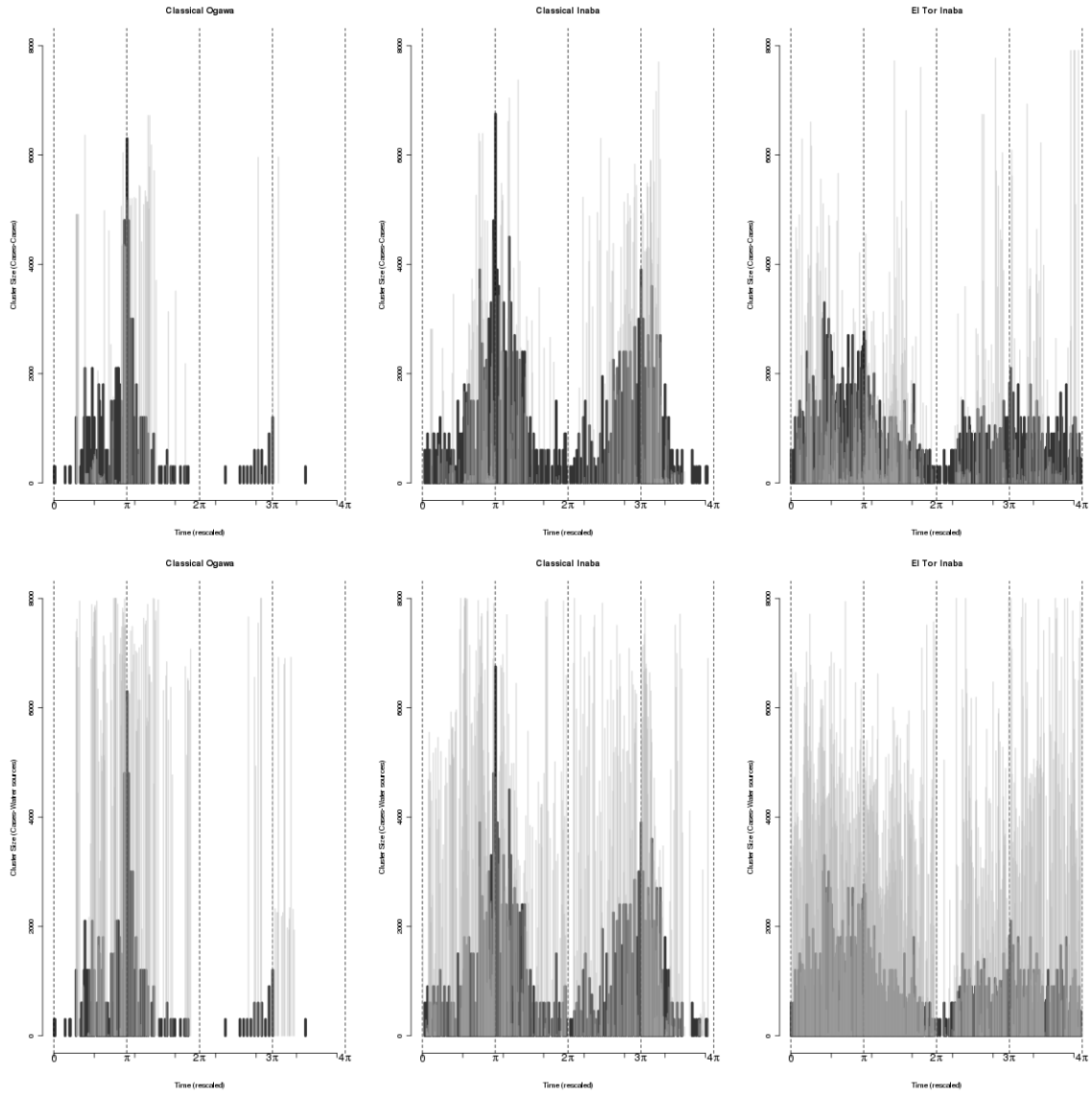


**Figure 3.6: Temporal dynamics of clustering and epidemic size.** Temporal dynamics of clustering and epidemic size averaged for all epidemics. Top row shows cluster size for cases in gray and epidemic size in black. Bottom row shows cluster size for cases-water in gray over epidemic size in black. Left column displays classical Ogawa data, center is classical Inaba and right column shows El Tor Inaba data.

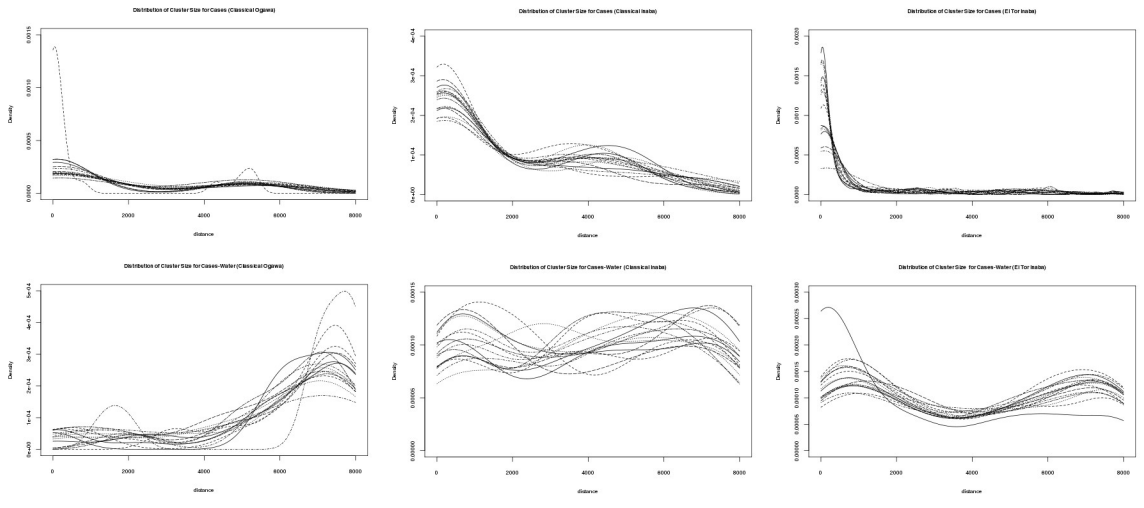


**Figure 3.7: Distribution of cluster sizes for different strains.** Top row shows cluster size for cases. Bottom row shows cluster size for cases-water. Left column displays classical Ogawa data, center is classical Inaba and right column shows El Tor Inaba data. Different lines represent different temporal aggregation of the data.

## Supplementary Material

**Table 3.S1:** Results for Kruskal-Wallis test for different time aggregation of the data, showing the difference between the distribution of cases during the fall  $[0-2\pi]$  and in the spring  $[2\pi-4\pi]$ .

Temporal Windows Size (days)	$\chi^2$	df	p-value
2	19.1725	1	1.194e-05
3	20.6864	1	5.41e-06
4	17.1092	1	3.529e-05
5	22.4301	1	2.179e-06
6	75.3018	1	< 2.2e-16
7	21.5255	1	3.492e-06
8	20.5482	1	5.815e-06
9	20.0848	1	7.408e-06
10	27.7922	1	1.351e-07
11	53.9584	1	2.048e-13
12	16.9417	1	3.855e-05
13	20.8998	1	4.839e-06
14	50.559	1	1.156e-12
15	88.0762	1	< 2.2e-16
16	76.3242	1	< 2.2e-16
17	105.8511	1	< 2.2e-16

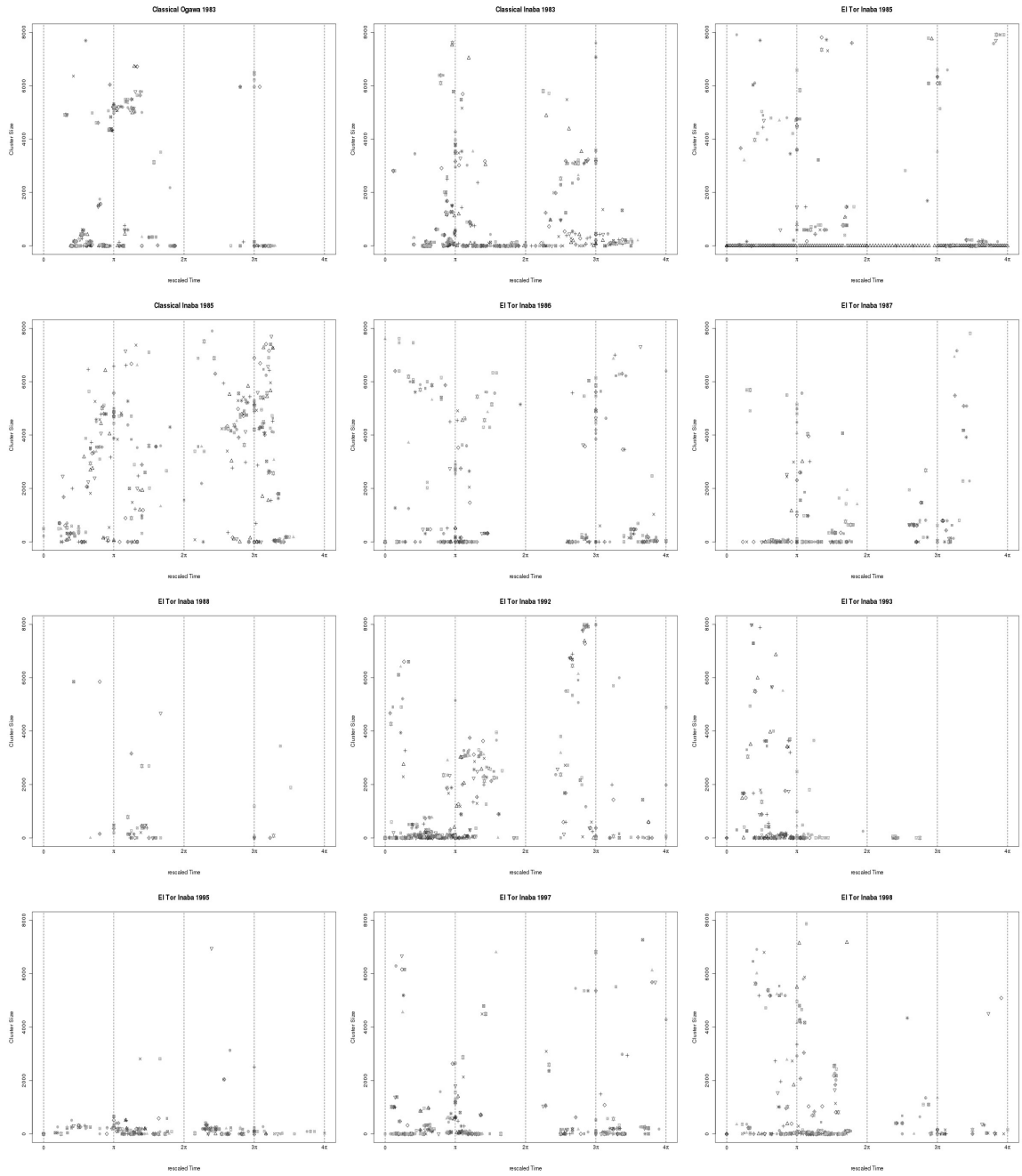


**Figure 3.S1: Clustering Size.** Each Figure shows the clustering size of cases for different epidemics. Different symbols represent different temporal aggregation of the cases.

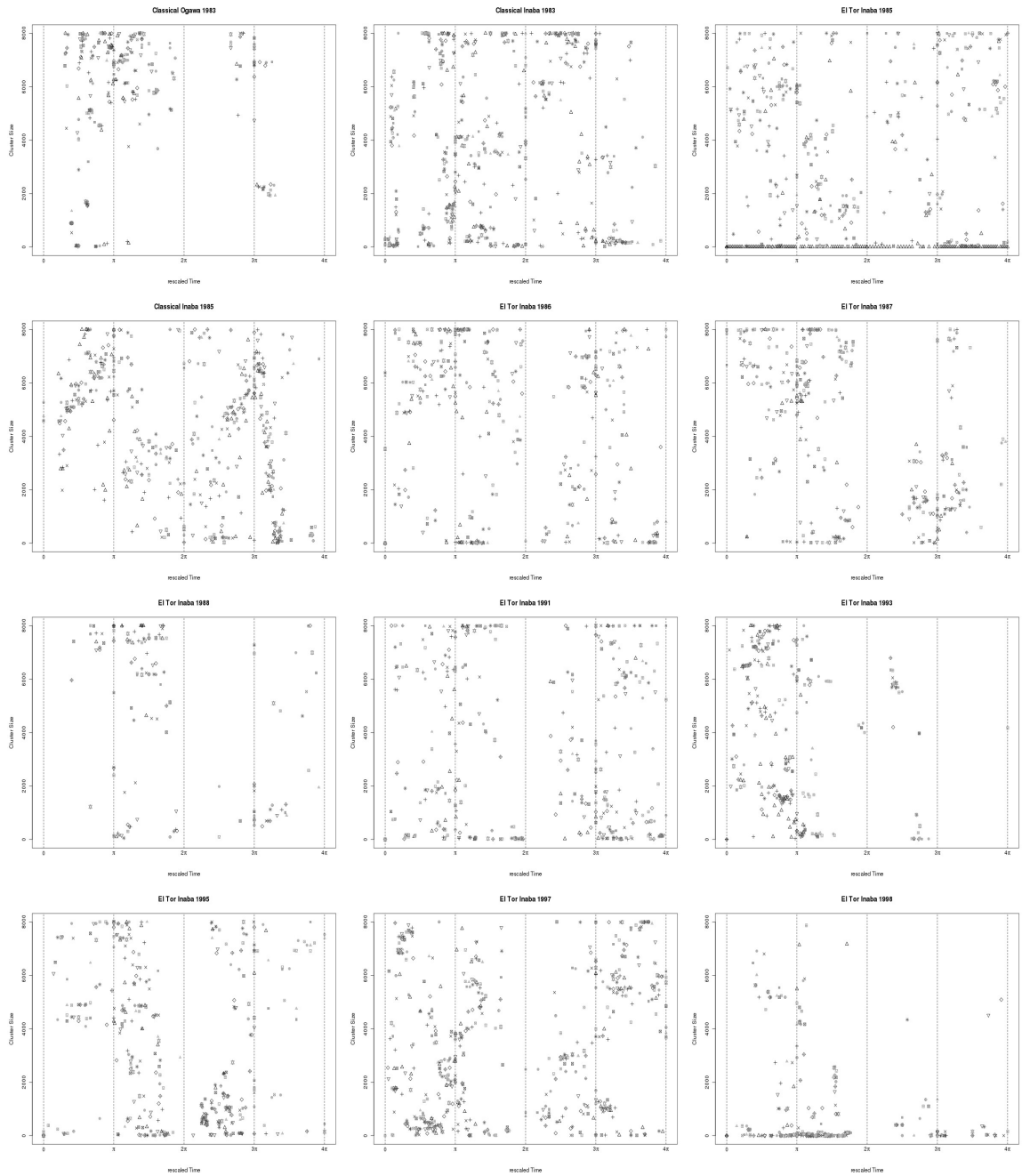


**Figure 3.S2: Clustering Size.** Each Figure shows the clustering size of cases-water for different epidemics. Different symbols represent different temporal aggregation of the cases.

## References

1. Grenfell BT, Bjørnstad ON, Kappey J: **Travelling waves and spatial hierarchies in measles epidemics.** *Nature* 2001, **414**:716—723.
2. Jolles AE, Sullivan P, Alker AP, Harvell CD: **Disease transmission of aspergillosis in sea fans: Inferring process from spatial pattern.** *Ecology* 2002, **83**:2373—2378.
3. Smith DL, Lucey B, Waller LA, Childs JE, Real LA: **Predicting the spatial dynamics of rabies epidemics on heterogeneous landscapes.** *Proceedings of the National Academy of Sciences* 2002, **99**:3668—3672.
4. Longini IM, Nizam A, Xu S, et al.: **Containing pandemic influenza at the source.** *Science* 2005, **309**:1083—1087.
5. Atti MLCD, Merler S, Rizzo C, et al.: **Mitigation measures for pandemic influenza in Italy: an individual based model considering different scenarios.** *PLoS ONE* 2008, **3**:e1790.
6. Ferguson NM, Cummings DAT, Fraser C, et al.: **Strategies for mitigating an influenza pandemic.** *Nature* 2006, **442**:448—452.
7. Snow J: *On the mode of communication of cholera.* London: John Churchill, New Burlington Street, England; 1855:139.
8. Miller CJ, Drasar B, Feachem RG: **Cholera and estuarine salinity in Calcutta and London.** *The Lancet* 1982, **319**:1216—1218.
9. Mooi FR, Bik EM: **The evolution of epidemic *Vibrio cholerae* strains.** *Trends In Microbiology* 1997, **5**:161—165.
10. Sack DA, Sack RB, Nair GB, Siddique AK: **Cholera.** *The Lancet* 2004, **363**:223—233.
11. Uma G, Chandrasekaran M, Takeda Y, Nair GB: **Recent advances in cholera genetics.** *Current Science* 2003, **85**:1538—1545.
12. Kaper JB, Morris JG, Levine MM: **Cholera.** *Clinical Microbiology Reviews* 1995, **8**:48—86.



13. Faruque SM, Sack DA, Sack RB, et al.: **Emergence and evolution of *Vibrio cholerae* O139**. *Proceedings Of The National Academy Of Sciences USA* 2003, **100**:1304—1309.
14. Koelle K, Pascual M, Yunus M: **Pathogen adaptation to seasonal forcing and climate change**. *Proc Biol Sci* 2005, **272**:971—977.
15. Reidl J, Klose KE: ***Vibrio cholerae* and cholera: out of the water and into the host**. *Fems Microbiology Reviews* 2002, **26**:125—139.
16. Blokesch M, Schoolnik GK: **Serogroup conversion of *Vibrio cholerae* in aquatic reservoirs**. *PLoS Pathogens* 2007, **3**:e81.
17. Pascual M, Bouma MJ, Dobson AP: **Cholera and climate: revisiting the quantitative evidence**. *Microbes and Infection* 2002, **4**:237—245.
18. Faruque SM, Islam MJ, Ahmad QS, et al.: **Self-limiting nature of seasonal cholera epidemics: Role of host-mediated amplification of phage**. *Proceedings Of The National Academy Of Sciences USA* 2005, **102**:6119—6124.
19. Ahmed MS, Raknuzzaman M, Akther H, Ahmed S: **The role of Cyanobacteria Blooms in Cholera Epidemic in Bangladesh**. *Journal of Applied Sciences* 2007, **13**:1785—1789.
20. King AA, Ionides EL, Pascual M, Bouma MJ: **Inapparent infections and cholera dynamics**. *Nature* 2008, **454**:877—880.
21. Ruiz-Moreno D, Pascual M, Bouma M, Dobson A, Cash B: **Cholera seasonality in Madras (1901-1940): Dual role for rainfall in endemic and epidemic regions**. *EcoHealth* 2007, **4**:52—62.
22. Glass RI, Becker S, Huq MI, et al.: **Endemic cholera in rural Bangladesh, 1966-1980**. *Am J Epidemiol* 1982, **116**:959—970.
23. Miller CJ, Feachem RG, Drasar BS: **Cholera Epidemiology in Developed and Developing Countries New Thoughts on Transmission, Seasonality, and Control**. *Lancet* 1985, **1**:261—263.
24. Craig M: **Time-space clustering of *Vibrio cholerae* 01 in Matlab, Bangladesh, 1970-1982**. *Soc Sci Med* 1988, **26**:5—13.

25. Huq A, Sack RB, Colwell RR: **Cholera and Global Ecosystems**. *Ecosystem change and public health: A global perspective* 2001, -:327—352.
26. Ali M, Emch M, Donnay JP, Yunus M, Sack RB: **The spatial epidemiology of cholera in an endemic area of Bangladesh**. *Social Science & Medicine* 2002, **55**:1015—1024.
27. Emch M: **Diarrheal disease risk in Matlab, Bangladesh**. *Social Science & Medicine* 1999, **49**:519—530.
28. Huq A, Sack RB, Nizam A, et al.: **Critical factors influencing the occurrence of Vibrio cholerae in the environment of Bangladesh**. *Appl. Environ. Microbiol.* 2005, **71**:4645-54.
29. Bailey TC, Gratell AC: *Interactive Spatial Data Analysis*. Prentice Hall; 1985.
30. Yamada S, Maskarinec G: **Strengthening PBL through a discursive practices approach to case-writing**. *Educ Health (Abingdon)* 2004, **17**:85—92.
31. Cazelles B, Stone L: **Detection of imperfect population synchrony in an uncertain world**. *Journal of Animal Ecology* 2003, **72**:953-968.
32. Pascual M, Rodo X, Ellner SP, Colwell RR, Bouma MJ: **Cholera dynamics and El Niño-Southern Oscillation**. *Science* 2000, **289**:1766—1769.
33. Russell CA, Smith DL, Childs JE, Real LA: **Predictive Spatial Dynamics and Strategic Planning for Raccoon Rabies Emergence in Ohio**. *PLoS Biology* 2005, **3**:e88—.
34. Earn DJ, Levin SA, Rohani P: **Coherence and conservation**. *Science* 2000, **290**:1360—1364.
35. Koelle K, Pascual M, Yunus M: **Serotype cycles in cholera dynamics**. *Proc Biol Sci* 2006, **273**:2879—2886.
36. Bouma MJ, Pascual M: **Seasonal and interannual cycles of endemic cholera in Bengal 1891-1940 in relation to climate and geography**. *Hydrobiologia* 2001, **460**:147-156.

37. Ferrari MJ, Grais RF, Bharti N, et al.: **The dynamics of measles in sub-Saharan Africa.** *Nature* 2008, **451**:679—684.
38. Finkenstädt BF, Grenfell BT: **Time series modelling of childhood diseases: a dynamical systems approach.** *Journal of the Royal Statistical Society: Series C (Applied Statistics)* 2000, **49**:187-205.
39. Grenfell BT, Harwood J: **(Meta)population dynamics of infectious diseases.** *Trends In Ecology & Evolution* 1997, **12**:395—399.
40. Grenfell BT, Wilson K, Finkenstadt BF, et al.: **Noise and determinism in synchronized sheep dynamics.** *Nature* 1998, **394**:674—677.
41. Ionides EL, Bretó C, King AA: **Inference for nonlinear dynamical systems.** *Proceedings Of The National Academy Of Sciences USA* 2006, **103**:18438—18443.
42. Rohani P, Earn DJ, Finkenstädt B, Grenfell BT: **Population dynamic interference among childhood diseases.** *Proc Biol Sci* 1998, **265**:2033—2041.
43. Rohani P, Earn DJ, Grenfell BT: **Impact of immunisation on pertussis transmission in England and Wales.** *Lancet* 2000, **355**:285—286.

## Chapter 4.

### A metapopulation approach for cholera dynamics in endemic areas

#### Background

Seasonality is present in the dynamics of most infectious diseases. Despite its ubiquitous nature and its importance to explaining and predicting the timing of epidemics, the seasonality of many infectious diseases is still poorly understood [1]. This is the case for cholera, an acute diarrheal infectious disease caused by the bacterium *Vibrio cholerae* that continues to be life-threatening especially in developing countries, and whose seasonality in endemic areas of Bangladesh exhibits two peaks per year and differs from that of other diarrheal diseases [2]. Such seasonal patterns can only be understood in the context of the different routes of transmission of the disease.

Two routes of transmission have been proposed for cholera [3, 4]. Primary or environmental transmission, by which new infections occur from contaminated water sources regardless of previous levels of infection and, secondary or human-to-human transmission, which links current levels of infections with previous levels on infection in the population and occurs via the fecal-oral route [2-4].

Early in 1985, Miller and colleagues proposed that primary transmission is responsible for the beginning of the seasonal epidemics [4]. Thus, in locations where only

one yearly epidemic peak is observed (such as Africa and Brazil), the beginning of epidemics has been associated with environmental conditions that favor the growth of the bacterium [5-8]. More complex explanations have been proposed for locations in Bangladesh, where two peaks occur each year before and after the monsoonal rains. These explanations include the population control of bacterial density by bacterio-phages [9-11], different survival strategies of the bacteria (including non culturable states) [12-14], the protection of bacterial populations by means of biofilm formation [15, 16] or the attachment to blue green algae [17]. All these mechanisms can be seen as exerting a bottom-up control on the occurrence of epidemics. However, more recently, human-to-human transmission and epidemiological factors, especially temporary immunity of the host, have been emphasized as playing an important role in modulating the size of epidemics [2, 9, 18-22]. This view consists of top-down mechanisms through the population dynamics of the disease. These different types of control suggest different hypotheses for the factors that are important to cholera dynamics in endemic areas.

Together with epidemiological characteristics, the spatial structure of the susceptible population may play an important role in determining the timing and severity of epidemics [23-25]. Although well mixed models have provided good approximations to explain the interannual variability of cholera dynamics at regional levels [2, 9, 18, 21, 26-29], it is not clear whether and how seasonality and transmission pathways influence the dynamics at higher spatial resolutions. Spatio-temporal patterns provide an opportunity to better understand routes of transmission, and in so doing, also better

understand seasonal mechanisms.

For diseases with extensive spatio-temporal data, models that relax the mean field approximation, have been developed to address patterns of transmission in detail. For example, at the level of cities and towns, measles dynamics in the UK was shown to spread in waves from bigger cities into smaller towns where stochastic extinction of the disease plays an important role [30]. Another example is the advance of the epidemic front for rabies in raccoons in USA, where Smith and colleagues found support for a role of the heterogeneity of the landscape and possibly (artificial) long distance movement of infected hosts [31, 32]. For cholera, questions on transmission mechanisms, on the importance of primary and secondary transmission, require consideration of smaller spatial scales than the ones considered so far in these previous studies. This requires in turn a different modeling approach. The spatio-temporal dynamics of the disease is considered here at the scale of households with a metapopulation approach that considers not just the propagation of the disease, as in the rabies front, but also the development of immunity behind this front.

The high resolution of the data used in this study allows us to investigate the seasonality of the two routes of transmission, and to address the importance of local (i.e., spatially restricted) transmission. In this endemic area in Bangladesh, the importance of local transmission has been suggested by clustering patterns in the data [3]; however, well-mixed models have also been used at the aggregated level of the whole population [9, 18, 21, 26, 29, 33]. Mean field models may be applicable because the abundance of

water sources might effectively break down the spatial structure of transmission.

Mathematical models of infectious diseases can help us understand the processes underlying the dynamics of epidemics [34]. Competing hypotheses describing epidemiological processes in detail can be used to formulate different models, and the goodness of fit of each of these models can be evaluated by calculating their likelihood given the data [35]. The “best” model can be selected by comparing the goodness of fit for each model in a way that takes into account the complexity of the model [36, 35].

We applied here a Bayesian approach to evaluate the role of both primary and secondary transmission in the dynamics of cholera in the endemic area of Matlab, Bangladesh. In addition to mean field models, with random mixing between susceptible and infected individuals, we also considered models incorporated local transmission. These models included infection of primary (environmentally driven) and/or secondary (human-to-human) origin. Both routes of transmission were allowed to exhibit different and independent seasonal patterns, because different factors such as climate and behavior might underlie this variability.

Results suggest that although both routes of transmission are dynamically important to the persistence of cholera, secondary transmission is the main epidemiological process during epidemics. Primary transmission appears to play a more limited role and to be most important for disease persistence and for the initiation of the seasonal outbreaks. Our results also suggest that transmission occurs at global levels, and

therefore that control strategies at the level of the whole region should be considered for reducing incidence in this area.

### **Methods and data**

Epidemiological data from the rural area of Matlab, Bangladesh, from 1983 to 2004 were used for this study. Matlab is located approximately 55 km south-east from the capital of the country (Figure 4.1). Adjacent to the confluence of the Meghna and Ganges rivers and bisected by the Dhonagoda river, this densely populated area is extremely flat, flooded periodically during the monsoon season (June-August approximately) and with a myriad of water ponds and water channels [37].

Human settlements in this area consist of groups of patrilineally related households, also known as *baris*, that share cooking and sanitary (mostly latrines) facilities [38]. Since 1994, baris were identified by a unique identification number, by the ICDDR (International Centre for Diarrhoeal Disease Research, Bangladesh), and hospitalized confirmed cholera cases were linked to the specific bari locations [38, 37], back to 1983. Additionally, information related with the average level of education (for 1994) for each location was obtained [39]. It is important to notice that untreated surface water from ponds and rivers is used by villagers for all household uses [40], since water from tube wells has been found to be contaminated with arsenic (studies reported that approximately 93% of the tube wells are contaminated [41]). Also, the fact that the Matlab hospital is the only treatment center in the area, and that it provides free treatment



to all patients, supports the assumption that reporting rates for this disease are high.

The analyses presented in this work focus on 18 years of cholera cases, from the beginning of 1985 to the end of 2003, for the 8340 baris in this database. During this period, 5033 cholera cases (O1 El Tor) were confirmed. Temporal variability is evident at both seasonal and inter-annual scales in the data (Figure 4.2). These cases were used to fit a set of models of increasing complexity.

The models were designed to analyze the role of primary and secondary transmission and incorporated the presence of interannual climate variability in the form of ENSO (the El Niño Southern Oscillation). The reemergence of cholera in Peru in 1991-2, during a strong ENSO event, motivated the hypothesis that ENSO could be a driver of cholera dynamics [14, 42]. This idea was tested for endemic areas in Bangladesh, and ENSO was found to explain at least 40% of the variability observed for the interannual patterns of cholera outbreaks [2, 26, 27].

Given that the spatial resolution (i.e., grain) of the data is at the level of baris, cholera epidemics were modeled at this level. Thus, baris are classified in one of three possible states, corresponding to susceptible (S), infected (I) or recovered (R). Because it is unlikely that a bari can gain complete immunity (i.e., to have all the inhabitants being in the recovered class), and even in such a case, cholera immunity is known to be temporary [43, 44, 18, 45], the recovered state assumed to also be temporary. Hence, recovered baris become susceptible again. A bari was considered to be in the infected class whenever a single case was reported for that particular location. The infectious

period for cholera cases has been suggested to last somewhere between 5 and 14 days [43, 44, 2, 46]. Thus infected baris, where recurrent cases were present within a two-weeks period, were assumed to remain in the infected state. All together, these assumptions lead to a set of SIRS models, where the unobserved transitions  $I \rightarrow R$  and  $R \rightarrow S$  were considered to be described by rates  $\nu$  and  $\gamma$  respectively, and the (only) observed transition,  $S \rightarrow I$ , is assumed to be the result of primary and/or secondary transmission, with seasonality included in both routes. In one of the models, secondary transmission inter-annually is a function of ENSO. Because transmission (especially but not restricted to the case of human-to-human transmission) might be a localized process, a spatially explicit model was also developed.

The models (for a detailed description and nomenclature see Table 4.1) included, two basic level models where only one route of transmission is allowed ( $P_{SIRS}$ , for primary transmission and  $S_{SIRS}$ , for secondary). The more elaborated models included: both routes of transmission ( $PS_{SIRS}$ ), seasonality (in one or both routes of transmission,  $(P^S)_{SIRS}$ ,  $(S^S)_{SIRS}$ ,  $(P^S)S_{SIRS}$ ,  $P(S^S)_{SIRS}$ ,  $(PS)^S_{SIRS}$ ), the influence of ENSO ( $PS^{S+ENSO}_{SIRS}$ ), and a localized transmission term ( $PS^{S+ENSO}_{SPATIAL}$ ). Finally, because differential susceptibility may play an important role in the dynamics of cholera in this region, an additional model, where the level of education of each bari affected the different rates of the disease, was included in these analyses ( $EDU_{SIRS}$ ).

Because of the existence of unobserved events, the fit of the parameters and likelihood calculation for these models is not trivial. For this kind of problems however, a

Markov Chain Monte Carlo (MCMC) approach can be used to recover the distribution of the underlying parameters [36]. This approach produces Markov chains of estimates that represent a random walk through the target (multivariate) distribution of the parameters. For each model, an initial state is generated assuming values for each parameter (in this case, epidemiological parameters were drawn from a uniform distribution between 0 and 1, and seasonal factors were set to 1) and a complete sequence of events is generated by simulation, consisting of infection (observed), recovery and loss of immunity events (unobserved, but simulated in concordance with the current parameter values) describing the data. Once this initial state is obtained, a new candidate state is constructed next using a Gibbs sampler (Figure 4.3). This involves two steps, first, each parameter is allowed to vary following a random walk, obtaining a new set of candidate parameters. Second, a candidate sequence of events is proposed (Figure 4.4). Here, with equal probability, recovery and loss of immunity events can be added to the current sequence of events, or removed, or moved in time. This new candidate state, including the candidate sequence and the candidate parameters, is accepted with a probability given by:

$$p = \min \left\{ 1, \frac{L(\text{State}_{\text{candidate}}) \cdot q(\text{State}_{\text{candidate}}, \text{State}_{\text{current}})}{L(\text{State}_{\text{current}}) \cdot q(\text{State}_{\text{current}}, \text{State}_{\text{candidate}})} \right\}$$

where  $L(\text{State})$  is the likelihood for a particular state (this is the sequence of events given the parameters), and  $q(v, w)$  represents the conditional probability of reaching candidate state  $v$  conditional on the current state  $w$  (Figure 4.3 and 4.4, also see [36, 47] for more details). If the transition is accepted the candidate state becomes the current state, otherwise the candidate state is rejected and the current state remains unaltered.

This algorithm is repeated (by generating a new candidate state) until convergence for all the parameters is reached. Notice that although both the parameter values and the sequence of events may change, at each iteration only unobserved events (i.e., recovery and loss of immunity events) are allowed to vary.

Convergence was tested using the Gelman and Rubin's scale reduction factor [36]. This index compares the variance within and among chains. Thus for each model,  $J$  (Markov) chains starting from different initial conditions were produced, and convergence was evaluated using:

$$R = \sqrt{\frac{1}{G} \cdot \left( G - 1 + \frac{B}{W} \right)}$$

where  $G$  is the length of each chain,  $B$  is the variance between chains, and  $W$  is the variance within chains. Convergence is acceptable for values of  $R < 1.2$  (see [36] for details).

Once convergence is reached, a distribution for the parameters is obtained and the different moments (i.e., mean, variance) can be calculated. In this Bayesian framework, model selection can be implemented by using the *deviance information criterion* (DIC) value corresponding to each model [35, 48, 49]. The DIC can be seen as a generalization of other information criteria (like the Akaike information criterion, AIC, and Bayesian information criterion, BIC) where the goodness of fit of a model is penalized by its complexity (i.e., the number of parameters). As for AIC, the smaller the DIC values, the better the model; moreover DIC values are only valid for comparison (i.e., absolute values are not interpretable).

The calculation of DIC involves the calculation of the mean deviance,  $\bar{D}$ , and the deviance of the means  $D(\bar{\theta})$ . The deviance is defined as:

$$D(\theta) = -2 \cdot \log(\text{likelihood}(y|\theta)) + C$$

where  $y$  are the data and  $\theta$  the unknown parameters, the constant  $C$  cancels out in all the calculations that involve model comparison, and therefore does not need to be known. The mean deviance is calculated as  $\bar{D} = E[D(\theta)]$ . The DIC can be calculated as

$$DIC = 2 \cdot \bar{D} - D(\bar{\theta})$$

The effective number of parameters in the model is defined as  $p_D = \bar{D} - D(\bar{\theta})$ , and therefore DIC is some times expressed as  $DIC = p_D + \bar{D}$  [36, 48, 49].

## Results

After verifying convergence, the DIC values were calculated for each model. The parameter values used for the calculation of DIC extended the last 5% of the chains (given that, on average 100000 MCMC steps were required for convergence, the DIC values and the parameters' posterior distributions considered at least 5000 values). The DIC and mean epidemiological parameters estimated for the models can be seen in Table 4.2. It is clear from Table 4.2 that, the models can be roughly sorted into three groups using DIC as a model selection criterion.

Table 4.2 shows that a very poor fit was obtained for models that only considered secondary transmission. The models that have either primary or both (primary and secondary) transmissions, regardless of seasonality, improved the fit significantly. These

last models displayed relatively small differences in their DIC values. Finally, the top models were those that included an ENSO influence in the interannual variability. The models with local transmission and variability in susceptibility are also in the top set of models. For this three models, however, DIC values are relatively close to each other.

It is worth noticing that these three groups also display similar values of the other epidemiological characteristics. In particular, the models with poor likelihood exhibited on average a standard infectious period, of approximately two weeks, but long temporal immunity.

For the group of models with a moderate fit, a different epidemiological picture was obtained. On average, these models showed short infectious periods of less than a week, with long immune periods of approximately four months. Mechanistically, since primary transmission is able to reignite the epidemics, long infectious periods are not needed and also temporal immunity can be longer.

The models with relatively good likelihoods, also exhibited similar epidemiological characteristics. These presented very short infectious and immune periods, as well as pronounced seasonality.

For the spatial model, different transmission distances were tested. These included models with fixed values for the range of secondary transmission, including 1000, 5000, 10000, 15000, 20000 and 25000 meters. Models with this range as a free parameter were also tested. The best results among these spatial models were obtained for a free parameter range that converged to a value of approximately 2 Km, suggesting that local

transmission occurs at relatively short distances.

The model selected as best was the one with global mixing, primary and secondary transmission, and ENSO as covariate. Figure 4.5 shows the seasonal forcing obtained for this model. Two peaks for the forcing of primary transmission are observed in May-June and December-January. Only one peak, in November, is observed for the forcing corresponding to secondary transmission, however the level of the forcing remains high during the winter.

It is of interest to compare the force of infection for the two modes of transmission quantitatively [34]. The (weekly) force of infection corresponding to primary and secondary transmission for the best model is shown in Figure 4.6. The primary force of infection was small when compared to that of secondary infections (Figure 4.6).

## **Discussion**

Results provide evidence for both primary and secondary transmission in the dynamics of cholera in Matlab, Bangladesh during the 1985-2003 period. Moreover, primary and secondary transmission were found to play different roles in the epidemiology of cholera. Primary transmission appears to play a role in initiating [4] and bridging epidemics; it peaks in January and June about two months before the epidemic peaks (April and October) (Figures 4.5 and 4.6). Also, in agreement with previous works (among others, [4, 9, 21]), secondary transmission is the main force during epidemics, and it peaks in the fall when it provides an important positive feedback between current

and previous levels of infection.

Although the fitted models displayed different parameters, the duration of both the infectious period and the immunity is in the order of days for the best models (see Table 2). It is important to remember that the modeling unit are baris. Thus, a very short infectious period suggests that cholera cases might be rapidly recognized by individuals in the surrounding areas, possibly adapting their behavior. This would effectively act as an isolation measure, resulting in a reduction of the infectious period at the level of baris. A short immune period at this spatial scale, is in agreement with the fact that long biological immunity might be expressed only by infected individuals [9, 18], and hence baris are never biologically immune, but only behaviorally immune, given the reported levels of infection.

For the best model, the mean force of infection corresponding to secondary transmission suggests a central role for secondary transmission during the whole year. Primary transmission, on the other hand, seems to play a very weak role, except perhaps in a short window of a few weeks preceding the spring peak. Despite this weak role, primary transmission remains central to persistence of the disease in the long term, since extinction of the disease occurs both locally and globally. This is shown by the fact that the mean force of infection corresponding to primary transmission lies inside the variance interval for the force of infection of secondary transmission (Figure 4.6).

These results also provide support for the hypothesis that secondary transmission is the dominant force behind the dynamics of cholera in this endemic region. Primary



transmission would contribute to the re-ignition of epidemics after the marked decreases in incidence or extinctions. This suggests that during low incidence periods, in the monsoonal season, the pathogen survives the harsh environmental conditions (possibly through any or all of the many proposed strategies, [50, 14, 15, 17]) with primary transmission contributing to the initiation of the seasonal fall outbreak. Secondary transmission also appears to play a more relevant role during the fall peak, in agreement with the early hypotheses that post-monsoonal conditions, such as a breakdown in sanitary conditions and crowdedness, are dynamically important [2, 33, 19]. Secondary transmission appears to remain important during the less severe disease trough in the winter.

The best model also indicate an important role of ENSO in the modulation the interannual variability in accordance to previous findings with mean-field model. In this model, the ENSO signal was modeled as a year-long on/off switch. Previous work found that ENSO indices act with a 9 to 11 months lag in advance of the cholera outbreaks [26], with El Niño conditions in the winter increasing transmission in the following fall. Such lags remain to explore with this modeling approach.

The results from the spatially explicit model describe a similar picture, but this model only reaches a second place in the ranking. Initially, this suggest that spatial structure may be not as important as previously suggested [3, 39, 51]. However, the spatial kernel used in this study is uniform and symmetric and may be a poor representation of the spatial structure underlying disease transmission in Matlab. For example, transmission

following river networks has been shown to describe the propagation of an outbreak in an epidemiologically naive area in south Africa [52]. For endemic areas in Bangladesh, a more important contact network may be the one determined by family and social relationships (i.e., blood lines, commercial and religious activities). A more detailed exploration of the spatial dynamics of epidemics would be necessary to examine transmission networks modified by the landscape or by social factors.

Another subject that requires further study is the susceptibility of baris at different locations. Notice that the model that considers differential susceptibility of the locations based on education level was ranked between the top models. A more complex socioeconomic index might be a better proxy for the susceptibility of baris. However, information mapping social and economic status is not available at the same temporal resolution than reported cases, making such extensions difficult to consider.

It is important to point out that simulations results (not shown here) overestimate the observed dynamics. This might result from the role of asymptomatic individuals [53, 9]. In all the models presented here, baris with only asymptomatic individuals were classified as susceptible locations, which may lead to underestimating the force of infection, and other parameter may be inflated to compensate for this. Thus, overestimation of the epidemics in simulations is a plausible consequence of ignoring asymptomatic individuals. Effectively, incorporating the presence of asymptomatic individuals would reduce the size of the class S (susceptible locations) and increase the size of the class I (infective locations). A similar result may be obtained if additional

protection against the disease is obtained by means of partial immunity. This would increase the size of the class R (recovered locations) and reduce the size of S. Incomplete immunity (at the level of baris) or behavioral changes due to the presence of the disease in surrounding areas, are only two of the factors that could contribute to create this effect. Furthermore, variability in the reporting rate (ignored here) may bias the parameter values obtained in different ways, and therefore models that incorporate this variability should be further analyzed.

More elaborated models at the level of individuals and not baris (Individual or Agent Based Models) might be formulated in order to test hypotheses about more complex transmission networks and aspects of human behavior or socio-economic differences. Consideration of asymptomatic individuals, inclusion of mild cholera cases in the database and monitoring of the presence of the bacterium in the environment are probably the most important directions to improve the current models.

Finally, the results suggest that disrupting secondary transmission might be central for controlling outbreaks, therefore efforts in that direction should be prioritized (but see also [54]). An intriguing possibility is that given the dominant role of secondary transmission, the persistence itself of the environmental reservoir that sustains primary transmission depends on the feedback from secondary cases. The pathogenic form of the *V. cholerae* may only be sustained in the reservoir when secondary transmission operates. This hypothesis is beyond the scope of the current models but could be explored with formulations that explicitly take into account the link between these two transmission

pathways, that after all are only a convenient discretization of the two extremes of a continuum.

Model	Primary Transmission	Secondary Transmission	Seasonality on Primary Transmission	Seasonality on Secondary Transmission	ENSO factors	Localized Transmission
$P_{SIRS}$	X					
$S_{SIRS}$		X				
$(P^S)_{SIRS}$	X		X			
$(S^S)_{SIRS}$		X		X		
$PS_{SIRS}$	X	X				
$(P^S)S_{SIRS}$	X	X	X			
$P(S^S)_{SIRS}$	X	X		X		
$(PS)^S_{SIRS}$	X	X	X	X		
$(PS)^{S+ENSO}_{SIRS}$	X	X	X	X	X	
$PS^{S+ENSO}_{SPATIAL}$	X	X	X	X	X	X
$EDU_{SIRS}$	X	X	X	X	X	

**Table 4.1:** Models' Descriptions. All models belong into the SIRS (Susceptible, Infected, Recovered, Susceptible) framework. For all models,  $I \rightarrow R$  transitions are assumed to be described by the parameter  $\nu$ , whose reciprocal determines the average infectious period; and analogously  $R \rightarrow S$  transitions are described by the parameter  $\gamma$ .  $\beta_p$  is the transmission coefficient corresponding to primary transmission, and  $\beta_s$  is the one for human-to-human transmission.  $S$  and  $I$  represent the number of susceptible and infected locations respectively. The seasonality for each transmission route,

$Season_p(t)$  and  $Season_s(t)$ , is implemented by using a spline with 5 parameters and

$ENSO_f(t)$  is a square function with a high value during years that registered an ENSO

event and a low value otherwise. The nomenclature of the models is as follow: P

represents the presence of Primary transmission, and S of Secondary transmission; the

superindex S means that the (base) route of transmission (P, S or both, PS) is affected for seasonal factors. Analogously, superindex ENSO includes the influence of ENSO factors. The subindex SPATIAL is self explanatory. The transmission for the different models is below.

$$\begin{aligned}
P_{SIRS} &= \beta_p \cdot S \\
S_{SIRS} &= \beta_s \cdot S \cdot I \\
(P^S)_{SIRS} &= \beta_p \cdot S \cdot Season_p(t) \\
(S^S)_{SIRS} &= \beta_s \cdot S \cdot I \cdot Season_s(t) \\
PS_{SIRS} &= \beta_p \cdot S + \beta_s \cdot S \cdot I \\
(P^S)S_{SIRS} &= \beta_p \cdot S \cdot Season_p(t) + \beta_s \cdot S \cdot I \\
P(S^S)_{SIRS} &= \beta_p \cdot S + \beta_s \cdot S \cdot I \cdot Season_s(t) \\
(PS)_{SIRS}^S &= \beta_p \cdot S \cdot Season_p(t) + \beta_s \cdot S \cdot I \cdot Season_s(t) \\
PS_{SIRS}^{S+ENSO} &= [\beta_p \cdot S \cdot Season_p(t) + \beta_s \cdot S \cdot I \cdot Season_s(t)] \cdot ENSO_f(t)
\end{aligned}$$

In the spatial model, transmission for each bari is analogous to the  $(PS)^{S+ENSO}_{SIRS}$ , but only Infected locations within a distance  $\rho$  are considered. In the fitting of the spatial model, some variant were tested with  $\rho$  as a fixed (with values 1000, 5000, 10000, 15000, 20000, 25000 meters) and also as a free parameter.

The model  $EDU_{SIRS}$  divided the bari population into two classes for each epidemiological state:  $S_H, S_L, I_H, I_L, R_H,$  and  $R_L$ . With the subindex (H) indicating whether the bari has an education level over the mean or not (L). Details on the calculation of the education index can be found in [38].

Model	DIC	$\beta_p$	$\beta_s$	$\nu$	$\gamma$
$(PS)^{S+ENSO}_{SIRS}$	30584.79	0.0004308741 (8.045618e-05)	1.8926878797 (6.313042e-02)	0.5696813094 (1.4431e-02)	0.2072140481 (1.98134e-02)
$PS^{S+ENSO}_{SPATIAL}$	31721.98	0.001458347 (4.586865e-03)	0.573904716 (2.810619e-02)	0.543240032 (4.80497e-02)	0.239969078 (1.017482e-01)
$EDU_{SIRS (L)}$	37932.53	0.03643907 (0.015619636)	0.44669897 (0.019614697)	0.63671732 (0.00332006)	0.68957135 (0.093581067)
$EDU_{SIRS (H)}$		0.02049350 (0.017595676)	0.83171769 (0.166794520)	0.56730375 (0.009175232)	0.12168747 (0.037107117)
$(PS)^S_{SIRS}$	150952.81	0.002353504 (6.880076e-05)	0.294939098 (7.824162e-04)	0.510312012 (1.14489e-03)	0.008921822 (1.8241e-04)
$P_{SIRS}$	140923.98	0.0001202704 (5.037326e-06)	NA	0.4994834792 (1.26612e-02)	0.0228174001 (7.78607e-03)
$(P^S)_{SIRS}$	141091.74	0.0001166314 (6.024172e-06)	0.0126865811 (5.582066e-02)	0.4587629800 (1.95338e-03)	0.0318243326 (8.21102e-04)
$(P^S)_{SIRS}$	148333.49	0.005997574 (8.835013e-05)	NA	0.477520869 (1.50151e-03)	0.005489590 (7.6322e-05)
$P(S^S)_{SIRS}$	142852.63	0.00009155255 (8.939019e-06)	0.2409728 (4.431865e-02)	0.5203382 (2.00421e-02)	0.05144085 (1.29282e-02)
$PS_{SIRS}$	140474.38	0.0001230822 (2.067334e-06)	0.0175230572 (1.271897e-02)	0.5160989805 (1.66405e-02)	0.0394326502 (1.91378e-02)
$(S^S)_{SIRS}$	30042089.98	0.12690228 (4.272422e-05)	0.69979196 (5.364343e-05)	0.06381875 (1.19364e-06)	0.00892024 (1.37275e-05)
$S_{SIRS}$	14070253.65	0.34109255 (8.539331e-07)	0.97068981 (4.713106e-05)	0.06381875 (3.75872e-05)	0.00325439 (9.75666e-06)

**Table 4.2:** DIC and mean parameters values obtained. Mean (standard deviation)

reported for epidemiological parameters.

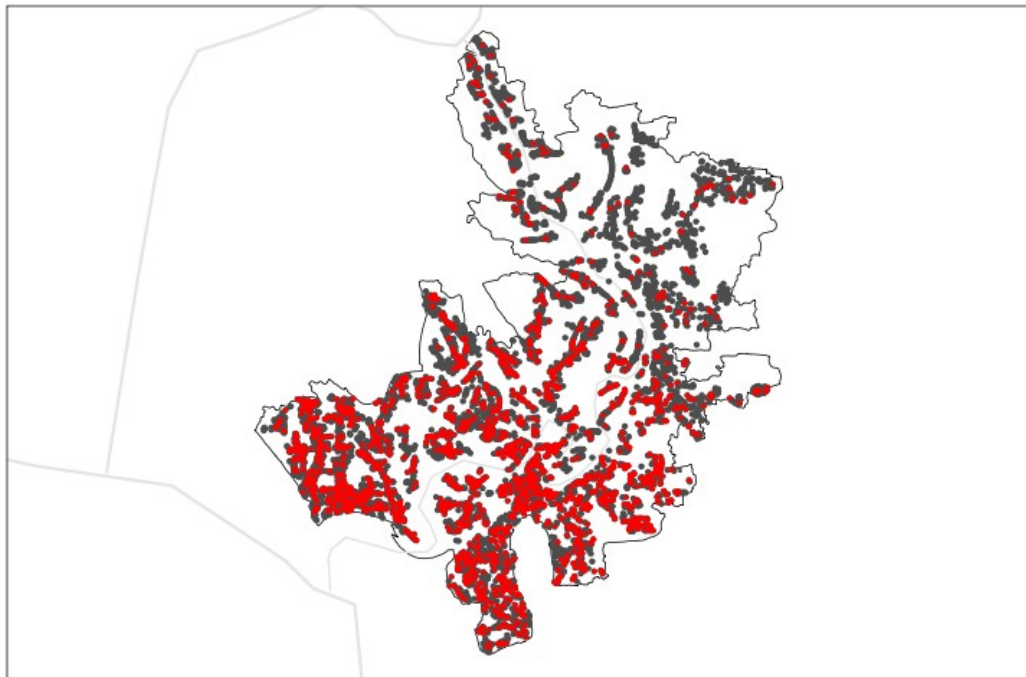


**Figure 4.1:** Spatial distribution of cholera cases during the period of study. The black dot represent the locations of the baris in Matlab, Bangladesh. The red point represent infections. Main rivers are showed as gray lines.



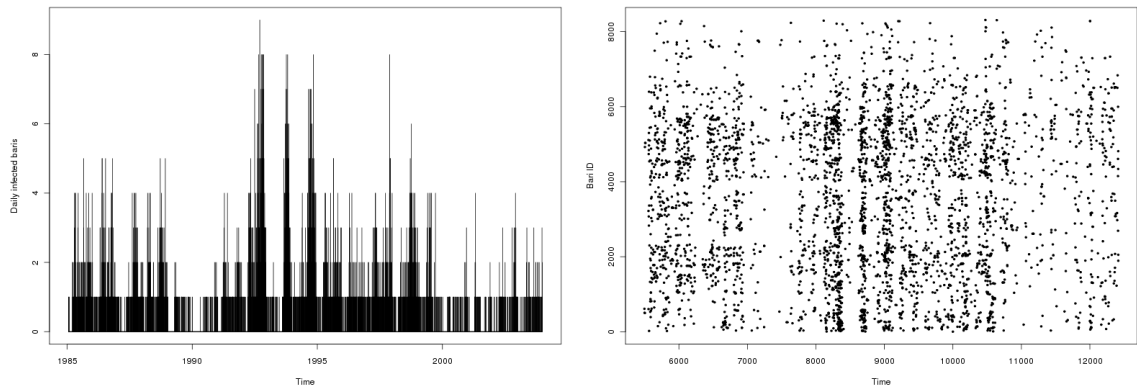


**Figure 4.2:** Temporal distribution of cases. On the left panel the time series of infected bars is shown. The dynamics for each location is showed in the panel on the right side.

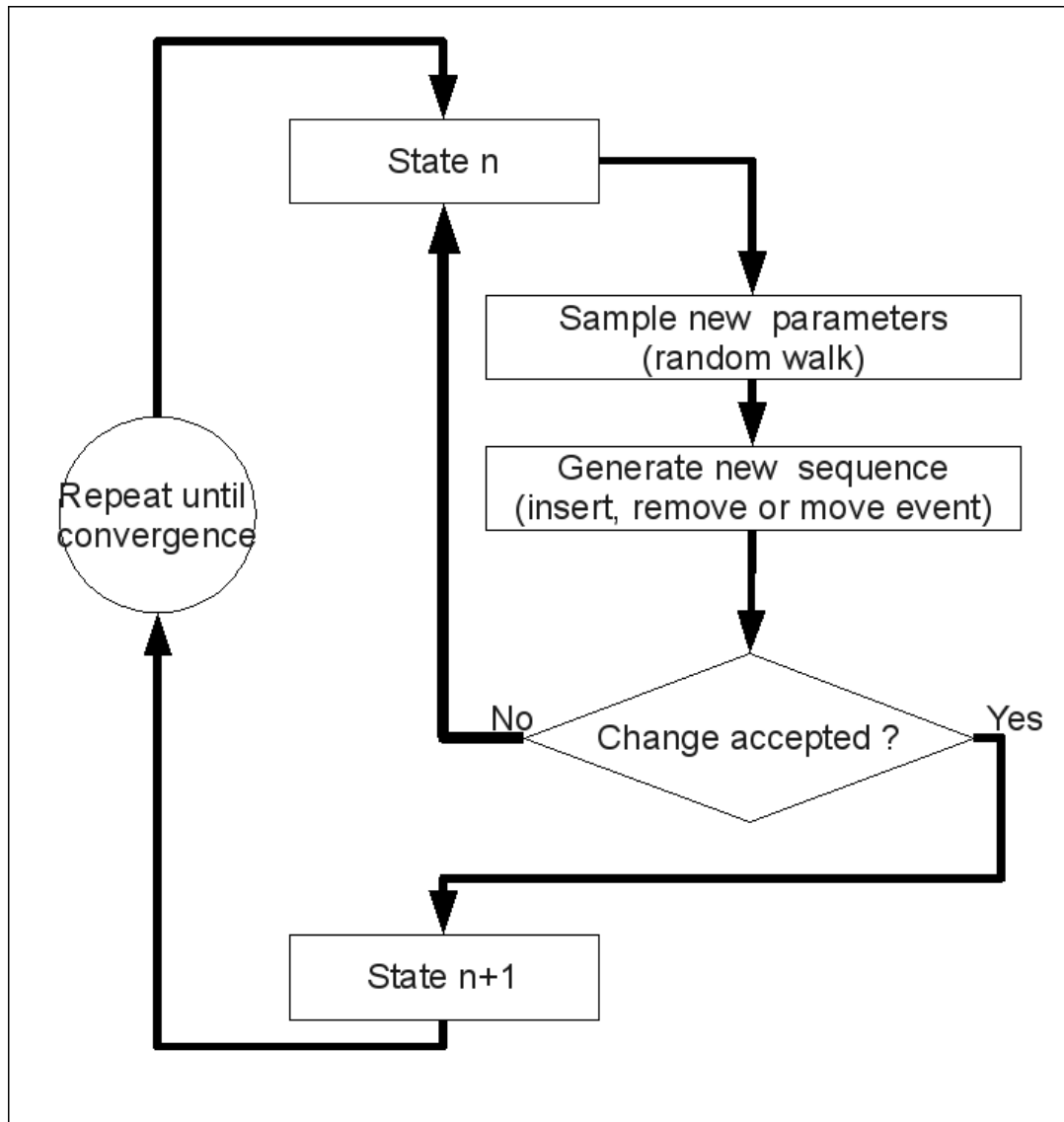


**Figure 4.3:** Each MCMC step involves moving from a state  $n$  (a set of parameters values and a sequence of events) to the next state  $n+1$ . This is done in two steps, first a new set of parameters is obtained and next a new sequence of events is generated. If the change is accepted, the state  $n$  becomes state  $n+1$  and the cycle starts again. Otherwise, the state  $n$  remains the same and a new state is proposed. This algorithm repeats until convergence is reached.

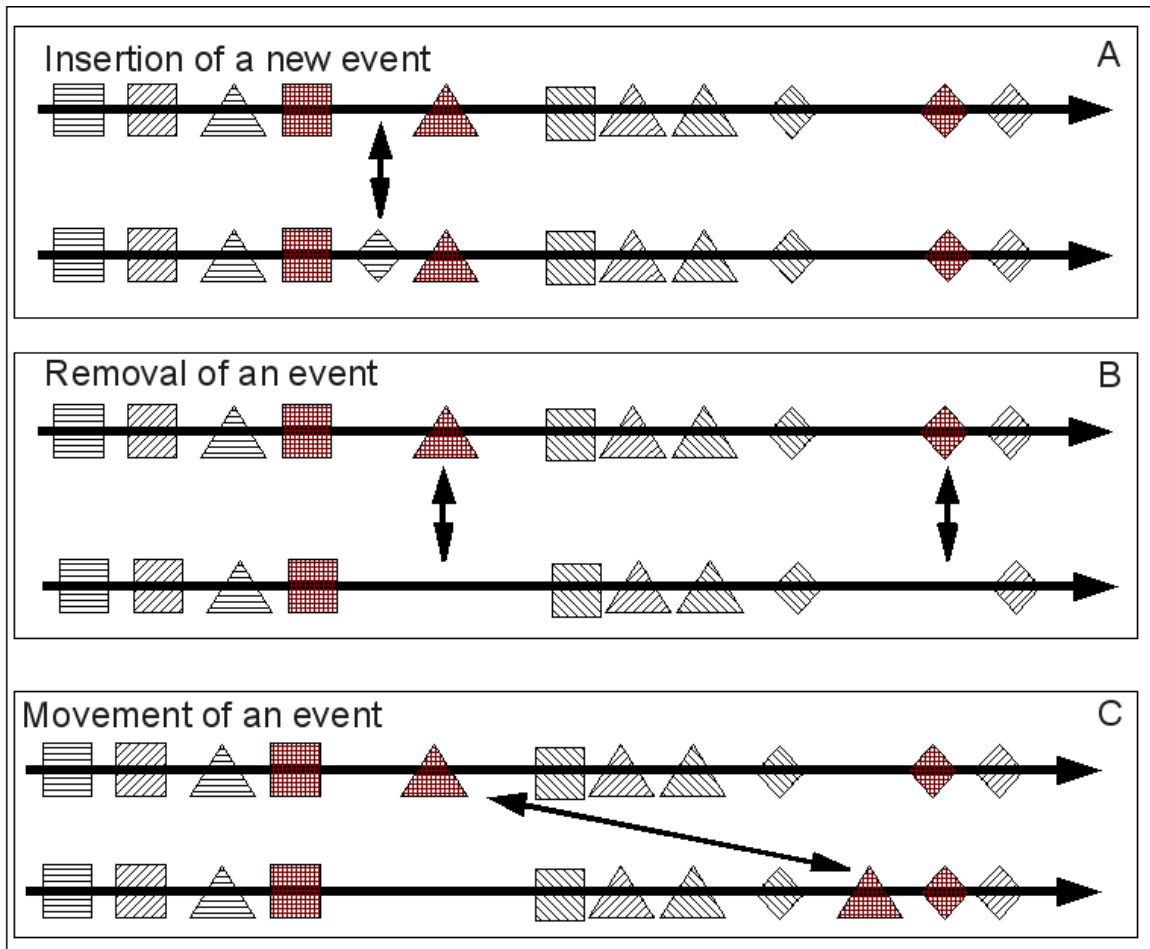


**Figure 4.4:** Creation of a new sequence. A new candidate sequence of events can be created by (A) inserting, (B) removing, or (C) moving an event. In each panel the current (above) and the candidate (below) sequence of events is shown. Squares indicate infection events, triangles represent recovery events and rhombus loss of immunity events. Different hatchings are used to represent different locations. Time flow is from left to right (thick black line). Double ended arrows are used to indicate the changes between current and candidate sequences.

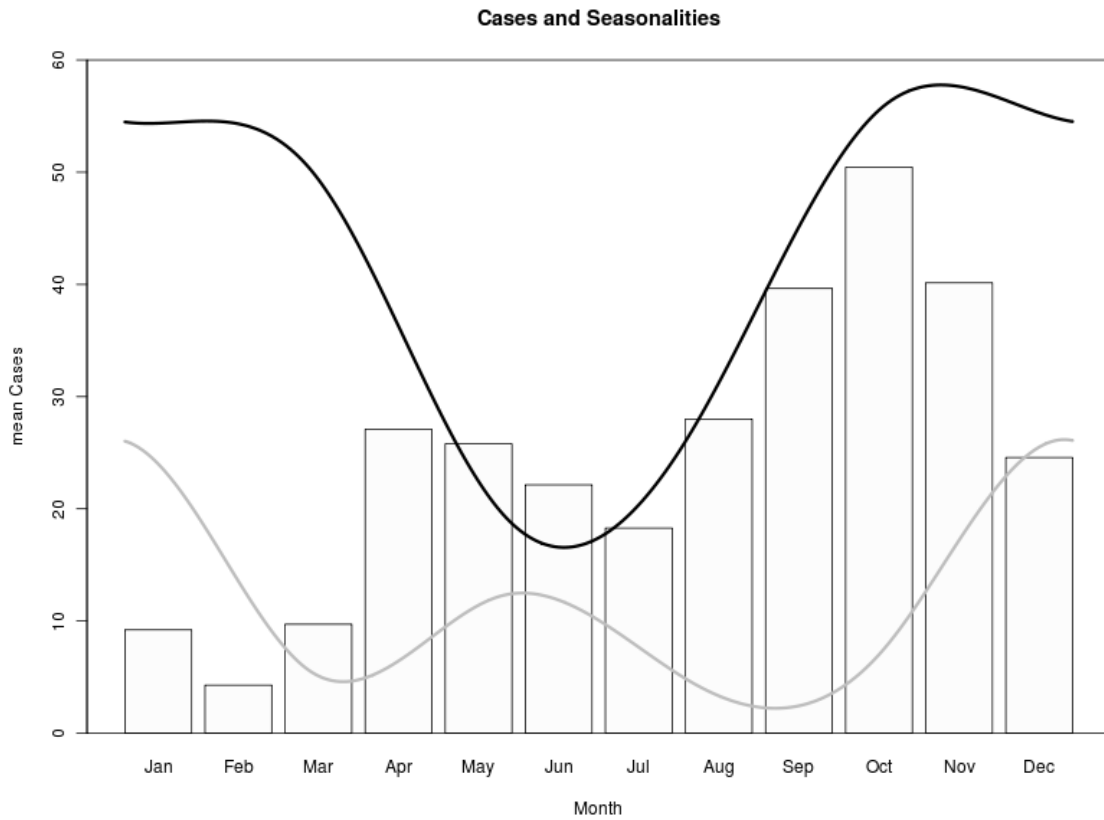


**Figure 4.5:** Average number of cases and seasonal forcing for primary and secondary transmission. Bars represent monthly average of infected baris. The lines represent the seasonal forcing obtained for both the primary and secondary route of transmission for the best model ( $PS^{S+ENSO}_{SIRS}$ ). Gray (black) line is the forcing for primary (secondary) transmission.

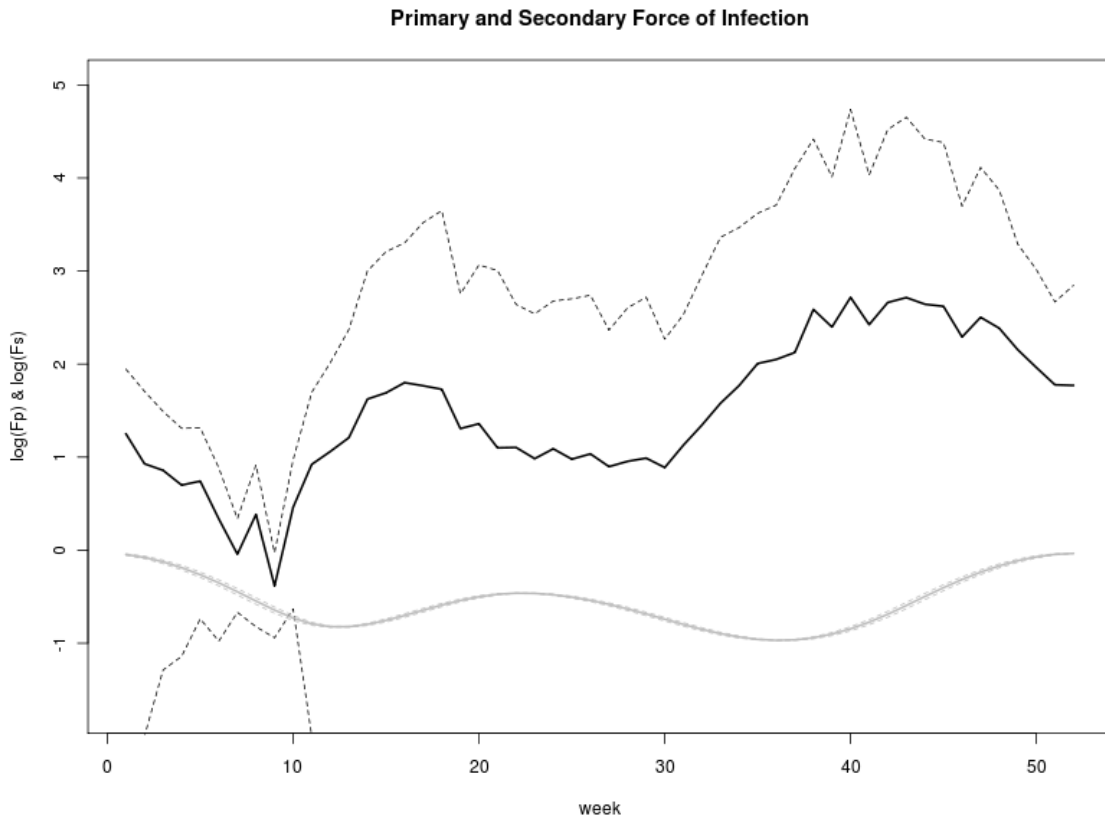


**Figure 4.6:** Force of Infection for primary ( $F_p$ ) and secondary ( $F_s$ ) transmission. The mean force of infection for secondary transmission (bold black line) was calculated by taking the average number of weekly new cases for each year (with dotted black line showing the variance). The mean and variance for the force of infection for primary transmission is shown in gray. A logarithmic scale is used to better show the variation of primary transmission.

## References

1. Fisman DN: **Seasonality of infectious diseases.** *Annu Rev Public Health* 2007, **28**:127—143.
2. Pascual M, Bouma MJ, Dobson AP: **Cholera and climate: revisiting the quantitative evidence.** *Microbes and Infection* 2002, **4**:237–245.
3. Craig M: **Time-space clustering of *Vibrio cholerae* 01 in Matlab, Bangladesh, 1970-1982.** *Social science & medicine (1982)* 1988, **26**:5-13.
4. Miller CJ, Feachem RG, Drasar BS: **Cholera Epidemiology in Developed and Developing Countries New Thoughts on Transmission, Seasonality, and Control.** *Lancet* 1985, **1**:261—263.
5. Codeço CT: **Endemic and epidemic dynamics of cholera: the role of the aquatic reservoir.** *BMC Infectious Diseases* 2001, **1**:1—1.
6. Glass R, Claeson M, Blake P, Waldman R, Pierce N: **Cholera in Africa - Lessons on transmission and control for Latin-America.** *Lancet* 1991, **338**:791-795.
7. Mintz ED, Guerrant RL: **A Lion in Our Village -- The Unconscionable Tragedy of Cholera in Africa.** *N Engl J Med* 2009, **360**:1060-1063.
8. Swerdlow DL, Greene KD, Tauxe RV, et al.: **Waterborne transmission of epidemic cholera in Trujillo, Peru: lessons for a continent at risk.** *The Lancet* 1992, **340**:28-32.
9. King AA, Ionides EL, Pascual M, Bouma MJ: **Inapparent infections and cholera dynamics.** *Nature* 2008, **454**:877—880.
10. Faruque SM, Islam MJ, Ahmad QS, et al.: **Self-limiting nature of seasonal cholera epidemics: Role of host-mediated amplification of phage.** *Proceedings Of The National Academy Of Sciences USA* 2005, **102**:6119—6124.
11. Faruque SM, Naser BI, Islam MJ, et al.: **Seasonal epidemics of cholera inversely correlate with the prevalence of environmental cholera phages.** *Proceedings of the National Academy of Sciences USA* 2005, **102**:1702—1707.
12. Colwell RR, Kaper J, Joseph SW: ***Vibrio cholerae*, *Vibrio parahaemolyticus*, and other vibrios: occurrence and distribution in Chesapeake Bay.** *Science* 1977, **198**:394-

6.

13. Colwell RR, Brayton PR, Grimes DJ, et al.: **Viable but nonculturable *V. cholerae* and related pathogens in the environment: Implications for release of genetically engineered microorganisms.** *Bio/technology* 1985, **3**:817—820.

14. Colwell RR: **Global climate and infectious disease: the cholera paradigm.** *Science* 1996, **274**:2025-31.

15. Heithoff DM, Mahan MJ: ***Vibrio cholerae* biofilms: Suck between a rock and a hard place.** *Journal Of Bacteriology* 2004, **186**:4835—4837.

16. Yildiz FH, Visick KL: ***Vibrio* biofilms: so much the same yet so different.** *Trends in Microbiology* 2009, **In Press, Corrected Proof.**

17. Islam MS, Drasar BS, Sack RB: **Probable role of blue-green algae in maintaining endemicity and seasonality of cholera in Bangladesh: a hypothesis.** *J Diarrhoeal Dis Res* 1994, **12**:245-56.

18. Koelle K, Rodo X, Pascual M, Yunus M, Mostafa G: **Refractory periods and climate forcing in cholera dynamics.** *Nature* 2005, **436**:696—700.

19. Ruiz-Moreno D, Pascual M, Bouma M, Dobson A, Cash B: **Cholera seasonality in Madras (1901-1940): Dual role for rainfall in endemic and epidemic regions.** *EcoHealth* 2007, **4**:52—62.

20. Hartley DM, Morris M, Smith DL: **Hyperinfectivity: A Critical Element in the Ability of *V. cholerae* to Cause Epidemics?** *PLoS Medicine* 2005, **3**:e7.

21. Koelle K, Pascual M: **Disentangling extrinsic from intrinsic factors in disease dynamics: A nonlinear time series approach with an application to cholera.** *American Naturalist* 2004, **163**:901—913.

22. Pascual M, Koelle K, Dobson AP: **Hyperinfectivity in Cholera: A New Mechanism for an Old Epidemiological Model?** *PLoS Medicine* 2006, **3**:e280—.

23. Anderson RM, May RM: *Infectious Diseases of Humans: Dynamics and Control.* Oxford University Press; 1991.

24. Bailey NTJ: *The Mathematical Theory of Infectious Diseases and Its Applications.*

1st edition. 1957:413.

25. Hudson PJ, Rizzoli A, Grenfell BT, Heesterbeek H, Dobson AP: *The Ecology of Wildlife Diseases*. 1st edition. Oxford University Press, USA; 2002.
26. Pascual M, Rodo X, Ellner SP, Colwell RR, Bouma MJ: **Cholera dynamics and El Niño-Southern Oscillation**. *Science* 2000, **289**:1766—1769.
27. Bouma MJ, Pascual M: **Seasonal and interannual cycles of endemic cholera in Bengal 1891–1940 in relation to climate and geography**. *Hydrobiologia* 2001, **460**:147-156.
28. Koelle K, Pascual M, Yunus M: **Pathogen adaptation to seasonal forcing and climate change**. *Proc Biol Sci* 2005, **272**:971—977.
29. Koelle K, Pascual M, Yunus M: **Serotype cycles in cholera dynamics**. *Proc Biol Sci* 2006, **273**:2879—2886.
30. Grenfell BT, Bjørnstad ON, Kappey J: **Travelling waves and spatial hierarchies in measles epidemics**. *Nature* 2001, **414**:716—723.
31. Russell CA, Smith DL, Childs JE, Real LA: **Predictive Spatial Dynamics and Strategic Planning for Raccoon Rabies Emergence in Ohio**. *PLoS Biology* 2005, **3**:e88—.
32. Smith DL, Lucey B, Waller LA, Childs JE, Real LA: **Predicting the spatial dynamics of rabies epidemics on heterogeneous landscapes**. *Proceedings of the National Academy of Sciences* 2002, **99**:3668—3672.
33. Pascual M, Dobson AP: **Seasonal Patterns of Infectious Diseases**. *PLoS Medicine* 2005, **2**:e5.
34. Keeling MJ, Rohani P: *Modeling Infectious Diseases in Humans and Animals*. 1st edition. Princeton University Press; 2007.
35. Hilborn R, Mangel M: *The Ecological Detective: Confronting Models with Data*. 1st edition. Princeton University Press; 1997.
36. Clark JS: *Models for Ecological Data: An Introduction*. illustrated edition. Princeton University Press; 2007.



37. Emch M: **Diarrheal disease risk in Matlab, Bangladesh.** *Social Science & Medicine* 1999, **49**:519—530.
38. Ali M, Emch M, Donnay JP, Yunus M, Sack RB: **The spatial epidemiology of cholera in an endemic area of Bangladesh.** *Social Science & Medicine* 2002, **55**:1015—1024.
39. Ali M, Emch M, Donnay JP, Yunus M, Sack RB: **Identifying environmental risk factors for endemic cholera: a raster GIS approach.** *Health Place* 2002, **8**:201-210.
40. Huq A, Sack RB, Nizam A, et al.: **Critical factors influencing the occurrence of Vibrio cholerae in the environment of Bangladesh.** *Appl. Environ. Microbiol.* 2005, **71**:4645-54.
41. Chowdhury AMR, Jakariya M: **Testing of Water for Arsenic in Bangladesh.** *Science* 1999, **284**:1621.
42. Epstein PR: **Algal blooms in the spreads and persistence of cholera.** *Biosystems* 1993, **31**:209—221.
43. Huq A, Sack RB, Colwell RR: **Cholera and Global Ecosystems.** *Ecosystem change and public health: A global perspective* 2001, -:327—352.
44. Kaper JB, Morris JG, Levine MM: **Cholera.** *Clinical Microbiology Reviews* 1995, **8**:48—86.
45. Sack DA, Sack RB, Nair GB, Siddique AK: **Cholera.** *The Lancet* 2004, **363**:223—233.
46. WHO: **Cholera, Fact Sheet N107.** - 2000, -:—.
47. Gibson GJ, Reshaw E: **Estimating parameters in stochastic compartmental models using Markov chain methods.** *IMA journal of mathematics applied in medicine and biology* 1998, **15**:19-40.
48. Spiegelhalter DJ, Best NG, Carlin BP, Linde AVD: **Bayesian Measures of Model Complexity and Fit.** *Journal of the Royal Statistical Society. Series B (Statistical Methodology)* 2002, **64**:583-639.
49. Lawson AB: *Bayesian Disease Mapping.* CRC Press; 2008:368.

50. Alam M, Sultana M, Nair GB, et al.: **Viable but nonculturable *Vibrio cholerae* O1 in biofilms in the aquatic environment and their role in cholera transmission.** *Proc. Natl. Acad. Sci. U.S.A.* 2007, **104**:17801-6.
51. Ali M, Emch M, Donnay JP, Yunus M, Sack RB: **The spatial epidemiology of cholera in an endemic area of Bangladesh.** *Soc Sci Med* 2002, **55**:1015-1024.
52. Bertuzzo E, Azaele S, Maritan A, et al.: **On the space-time evolution of a cholera epidemic.** *Water Resour. Res.* 2008, **44**:W01424.
53. Ionides EL, Bretó C, King AA: **Inference for nonlinear dynamical systems.** *Proceedings Of The National Academy Of Sciences USA* 2006, **103**:18438—18443.
54. Colwell RR, Huq A, Islam MS, et al.: **Reduction of cholera in Bangladeshi villages by simple filtration.** *Proceedings of the National Academy of Sciences of the United States of America* 2003, **100**:1051-1055.

## **Chapter 5.**

### **Conclusion**

The different chapters of this work analyzed cholera dynamics at a higher spatial resolution than ever done before, in relation to the question of different routes of transmission and their seasonality, and provided evidence for the fundamental differences between endemic and epidemic dynamics from the perspective of climate forcing, differences that intimately connect to both seasonality and routes of transmission. These analyses build on the current knowledge of the processes driving the dynamics of cholera and expand on the statistical analysis that include climatic variables [1-3], environmental variability [4, 5], and the importance of both intrinsic and extrinsic processes shaping the endemic dynamics [6-8].

Initially, the analyses on monthly cholera mortality in the Madras Presidency, allowed the identification of endemic and epidemic areas in this former British region. The statistical approach presented in Chapter 2, also indicated a dual role for rainfall, influencing positively the occurrence of disease outbreaks in epidemic areas, whereas negatively in the endemic areas. Finally, the correlations detected between cholera mortality and rainfall in this region provided initial insights on the different roles for primary and secondary transmission of cholera.

The link between climate variability and disease dynamics has been established not only for cholera [9, 2, 3] but also for other diseases [10-12]. In particular for Meningococcal meningitis, at the regional level in west Africa, the relationship between climatic factors and disease incidence opens the possibility for the development of an early warning system for the onset of epidemics, with clear implications for public health [10]. For cholera, this seems to be a much difficult task because of the interactions between epidemiological dynamics, primarily as a result of population 'herd' immunity and climate variability; however, advances in studying this interaction from time series data using statistical inference methods for nonlinear dynamical systems, are allowing progress in this area [7, 13, 14]. This work has been so far restricted to endemic areas; thus the differentiation of endemic and epidemic areas is important. The results of Chapter 2 suggest that responses to climate variability can involve different lags and potentially different signs, and therefore, the question of prediction for epidemic regions remains open and a subject for the future.

High resolution spatio-temporal data, like the extensive records analyzed in Chapters 3 and 4, provide an opportunity to better understand the seasonality of disease and different routes of transmission for diseases that involve not just the typical secondary route, from human to human, but also an environmental reservoir and external force of infection associated with it.

These models analyzed the extensive dataset corresponding to the last two decades of every reported case of cholera in Matlab, Bangladesh [15-18]. The first analysis

(Chapter 3) of this detailed dataset described the spatial patterns from a static statistical perspective [19]. Based on a similar approach used for the identification of specific routes of transmission for aspergillosis in sea fans [20], the spatial distribution of cholera cases was statistically tested for spatial aggregation. These analyses showed that cholera cases form clusters, supporting a central role of secondary transmission, whereas a fuzzy description was obtained for primary transmission (i.e., spatial aggregation of cases and water sources). The less conclusive result on aggregation of cases and water ponds, may be a consequence of incomplete information on water sources, and water usage.

Building on these (static) results, a dynamical approach was formulated.

Although, dynamical approaches for the metapopulation dynamics of infectious diseases are not new, the spatial resolution and type of model required for a disease like cholera, differ from what has been done before. For example, foot and mouth disease has been model using set of spatially coupled populations with transmission between them as a function of the local levels of infection [21]. Similarly, but still at a lower spatial resolution of towns, cities or other administrative units, measles and dengue ([22, 23]) were found to spread in a wave like pattern from specific areas. Fewer studies in the field of infectious diseases have treated units of study as being in one of a set of discrete states of the classical epidemiological models (i.e., susceptible, exposed, infective or recovered). This has been done for rabies [24, 25] to model the infection front that propagates in a wave like fashion and to identify irregularities in this propagation due to heterogeneities in the landscape. But again the spatial resolution was low, and the unit of study was at the

level of counties. Much finer resolutions have been considered instead in models for the spread of disease outbreaks in plants populations [26]. We have extended this approach to consider disease with temporary immunity. This adds one more unobserved state to a system where typically only one state is measured. We have also added seasonal variation in transmission and considered two different routes of transmission. Metapopulation research has for the most part ignored seasonal variation in the colonization process, which plays an analogous role to infection in disease dynamics [27]. The work presented in Chapter 4 considered the spatial unit of study to be a bari or group of households and could also be applied for finer units if data is reported at that level. Consideration of endemic dynamics with temporary immunity requires consideration not just of the front of infection and its propagation, but of back-propagation to regions behind the front where disease has already arisen.

A challenge in the analysis of epidemiological databases is the absence of information regarding recovery and loss of immunity events. It is solved here by using a Markov Chain Monte Carlo approach for fitting the family of models studied in Chapter 4. The output of these novel models, demonstrates the importance of both primary and secondary transmission in shaping the dynamics of endemic cholera.

In agreement with the results presented in Chapter 3, local transmission significantly improves the likelihood of the models. However, the best model corresponds to a spatially implicit one. This may be related to the simplicity of the spatial kernel used in this study which may be a poor representation of the spatial structure underlying

disease transmission in Matlab. A social contact network that dynamically adapts to the presence of the disease may be more adequate to represent a non-random mixing of susceptible and infected individuals in this study area. This contact network could also incorporate landscape features, such as rivers, that also may play a role in the spatial structure of transmission. A model that includes all this information will probably require to adopt an individual, or agent, based model approach.

Historically cholera epidemics, have exposed the lack of sanitary conditions in human communities [29]. Moreover, cholera models (including those developed in this work) showed that the complex transmission structure of the disease with two routes is partially responsible for the establishment of endemic regions. Control measures that target primary transmission have been suggested in the past and are clearly important from the perspective of disease persistence [30], however, the dominant role of secondary transmission identified in this work suggests that containment of secondary infections may be a viable and useful strategy to control epidemics. Perhaps more intriguing, is the possibility that secondary transmission is required for the persistence of the primary route itself, that is, for the persistence of the pathogenic form of the bacterium in the environment. Our model did not include explicit feedbacks between these two modes of transmission but future work should consider models and data that would allow an exploration of this dependence. After all, these two routes are two extremes of a continuum.

The approach presented here should be applicable to other infectious diseases for

which spatio-temporal data at high resolution becomes available. This type of data sets is likely to become more common with better surveillance systems and the increasing application of geographic information systems to epidemiology. In particular, the framework presented in Chapter 4 enables the study of data with incomplete information, when latent or hidden states are present. Furthermore, the approach could be easily adapted to model ecological systems using transitions between discrete states, analogous in a sense to the matrix approaches developed by Caswell for population ecology [31], to forest fire models [32] and those for stochastic vegetation dynamics [33], among others. The main limitation will be the trade-offs between the length and detail of the dataset and the capability to reach convergence in the method of parameter estimation.

The modeling approach presented here represents one more step forward to better understand, and therefore predict and may be control, cholera disease outbreaks, as well as other diseases that threaten human and wild life populations, at a time when more extensive data sets are becoming available. In ecology and epidemiology, data sets will be more extensive in time and space but will always be incomplete in representing the state of the system.



## References

1. Colwell RR: **Global climate and infectious disease: the cholera paradigm.** *Science* 1996, **274**:2025-31.
2. Pascual M, Rodo X, Ellner SP, Colwell RR, Bouma MJ: **Cholera dynamics and El Niño-Southern Oscillation.** *Science* 2000, **289**:1766—1769.
3. Russell AJH: **A statistical approach to the epidemiology of cholera in Madras Presidency.** *Proceedings Of The National Academy Of Sciences USA* 1925, **11**:653—657.
4. Atti MLCD, Merler S, Rizzo C, et al.: **Mitigation measures for pandemic influenza in Italy: an individual based model considering different scenarios.** *PLoS ONE* 2008, **3**:e1790.
5. Colwell RR, Kaper J, Joseph SW: **Vibrio cholerae, Vibrio parahaemolyticus, and other vibrios: occurrence and distribution in Chesapeake Bay.** *Science* 1977, **198**:394-6.
6. Koelle K, Pascual M: **Disentangling extrinsic from intrinsic factors in disease dynamics: A nonlinear time series approach with an application to cholera.** *American Naturalist* 2004, **163**:901—913.
7. Koelle K, Rodo X, Pascual M, Yunus M, Mostafa G: **Refractory periods and climate forcing in cholera dynamics.** *Nature* 2005, **436**:696—700.
8. Koelle K, Pascual M, Yunus M: **Pathogen adaptation to seasonal forcing and climate change.** *Proc Biol Sci* 2005, **272**:971—977.
9. Luque Fernández MÁ, Bauernfeind A, Jiménez JD, et al.: **Influence of temperature and rainfall on the evolution of cholera epidemics in Lusaka, Zambia, 2003-2006: analysis of a time series.** *Transactions of the Royal Society of Tropical Medicine and Hygiene* 2009, **103**:137-143.
10. Sultan B, Labadi K, Guégan J, Janicot S: **Climate Drives the Meningitis Epidemics Onset in West Africa.** *PLoS Med* 2005, **2**:e6.
11. Altizer S, Dobson A, Hosseini P, et al.: **Seasonality and the dynamics of infectious diseases.** *Ecol Lett* 2006, **9**:467—484.

12. Pascual M, Dobson AP: **Seasonal Patterns of Infectious Diseases.** *PLoS Medicine* 2005, **2**:e5.
13. Pascual M, Chaves LF, B. Cash, Rodo X, Yunus M: **Predicting endemic cholera: the role of climate variability and disease dynamics.** *CLIMATE RESEARCH* 2008, **36**:131-140.
14. King AA, Ionides EL, Pascual M, Bouma MJ: **Inapparent infections and cholera dynamics.** *Nature* 2008, **454**:877—880.
15. Ali M, Emch M, Donnay JP, Yunus M, Sack RB: **The spatial epidemiology of cholera in an endemic area of Bangladesh.** *Social Science & Medicine* 2002, **55**:1015—1024.
16. Ali M, Goovaerts P, Nazia N, et al.: **Application of Poisson kriging to the mapping of cholera and dysentery incidence in an endemic area of Bangladesh.** *International journal of health geographics* 2006, **5**:45.
17. Emch M: **Diarrheal disease risk in Matlab, Bangladesh.** *Social Science & Medicine* 1999, **49**:519—530.
18. Emch M, Feldacker C, Islam MS, Ali M: **Seasonality of cholera from 1974 to 2005: a review of global patterns.** *International journal of health geographics* 2008, **7**:31.
19. Bailey TC, Gratell AC: *Interactive Spatial Data Analysis.* Prentice Hall; 1985.
20. Jolles AE, Sullivan P, Alker AP, Harvell CD: **Disease transmission of aspergillosis in sea fans: Inferring process from spatial pattern.** *Ecology* 2002, **83**:2373—2378.
21. Keeling MJ, Woolhouse ME, Shaw DJ, et al.: **Dynamics of the 2001 UK foot and mouth epidemic: stochastic dispersal in a heterogeneous landscape.** *Science* 2001, **294**:813-817.
22. Cummings D, Irizarry R, Huang N, et al.: **Traveling waves in dengue hemorrhagic fever incidence in Thailand.** *JOURNAL OF CLINICAL VIROLOGY* 2003, **28**:S29-S29.
23. Grenfell BT, Bjørnstad ON, Kappey J: **Travelling waves and spatial hierarchies in measles epidemics.** *Nature* 2001, **414**:716—723.
24. Russell CA, Smith DL, Childs JE, Real LA: **Predictive Spatial Dynamics and**

**Strategic Planning for Raccoon Rabies Emergence in Ohio.** *PLoS Biology* 2005, **3**:e88—.

25. Smith DL, Lucey B, Waller LA, Childs JE, Real LA: **Predicting the spatial dynamics of rabies epidemics on heterogeneous landscapes.** *Proceedings of the National Academy of Sciences* 2002, **99**:3668—3672.

26. Gibson GJ, Reshaw E: **Estimating parameters in stochastic compartmental models using Markov chain methods.** *IMA journal of mathematics applied in medicine and biology* 1998, **15**:19-40.

27. Grenfell BT, Harwood J: **(Meta)population dynamics of infectious diseases.** *Trends In Ecology & Evolution* 1997, **12**:395—399.

28. Hilborn R, Mangel M: *The Ecological Detective: Confronting Models with Data.* 1st edition. Princeton University Press; 1997.

29. Kaper JB, Morris JG, Levine MM: **Cholera.** *Clinical Microbiology Reviews* 1995, **8**:48—86.

30. Colwell RR, Huq A, Islam MS, et al.: **Reduction of cholera in Bangladeshi villages by simple filtration.** *Proceedings of the National Academy of Sciences of the United States of America* 2003, **100**:1051-1055.

31. Caswell H: *Matrix Population Models: Construction, Analysis, and Interpretation.* 2nd edition. Sinauer Associates; 2000.

32. Boychuk D, Braun W, Kulperger R, Krougly Z, Stanford D: **A stochastic forest fire growth model.** *Environmental and Ecological Statistics* 2009, **16**:133-151.

33. Balzter H: **Markov chain models for vegetation dynamics.** *Ecological Modelling* 2000, **126**:139-154.